Charles University

Faculty of Mathematics and Physics

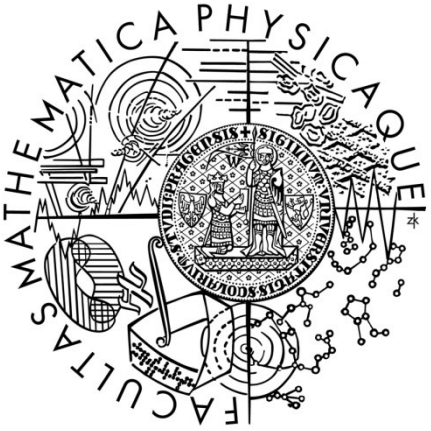

HABILITATION THESIS

Mgr. Ivan Khalakhan Ph.D.

Platinum-based bimetallic cathode catalysts for proton-exchange membrane fuel cells

Prague 2020

Acknowledgements

Since the very nature of scientific work is cooperation the results presented in this thesis could not be accomplished without the valuable contributions of many colleagues with whom I have worked, collaborated, or discussed. I would like to express my gratitude to all my colleagues from the Department of Surface and Plasma Science of Charles University with a special mention to Prof. Vladimír Matolín and Prof. Iva Matolínová. I wish to further thank all co-authors for their very friendly and always helpful collaboration.

I am also grateful for the opportunity to be a part of Supermolecules Group of National Institute for Material Science (Tsukuba, Japan) and Institute for Inorganic Chemistry, Graz University of Technology (Graz, Austria) during my internships.

Last but not least, I want to thank my family and friends, for the continuous support and motivation.

Contents

Preface

Presented habilitation thesis is focused on the investigation of platinum catalysts and platinum-based bimetallic alloys prepared by magnetron sputtering for application to the cathode side of hydrogen powered proton-exchange membrane fuel cells (PEMFC). Advanced *in situ/in operando* experimental methods and techniques such as an electrochemical cell (EC) coupled with atomic force microscopy (AFM), grazing incidence small angle X-ray scattering (GISAXS), inductively coupled plasma mass spectrometry (ICP-MS), infrared reflection absorption spectroscopy (IRRAS) and near-ambient pressure X-ray photoelectron spectroscopy (NAP-XPS) are used to probe relationships between the structure, composition, stability of catalytic materials and their ORR reactivity. The main goal of the thesis is to directly explore the physics and chemistry behind the activity and durability of the cathode catalysts prepared by magnetron sputtering in real PEMFCs.

The work is comprised of an annotated collection of own works. The presented research was conducted at several institutions and research infrastructures, namely, Department of Surface and Plasma Physics at Faculty of Mathematics and Physics of Charles University, Department of Chemistry and Pharmacy of Friedrich-Alexander-Universität Erlangen-Nürnberg (Erlangen, Germany), Helmholtz-Institute Erlangen-Nürnberg for Renewable Energy (Erlangen, Germany), Department of Materials Science and Physical Chemistry, Institute of Theoretical and Computational Chemistry of the University of Barcelona (Barcelona, Spain), Chalmers University of Technology (Gothenburg, Sweden) and the Synchrotron Elettra (Trieste, Italy).

1. Background

1.1. "Green" energy

Recent climate changes, a massive boost in global energy consumption, and the depletion of fossil energy sources faced humanity either shrinking economy or reducing reliance on fossil fuels through harvesting low or even zero-emission energy. The latter is seen as a priority option. Moreover, the development of renewable energy technology has now advanced enough to realize this ambitious idea. In this regard, the European Council in December 2019 endorsed the European Union ground-breaking target of approaching towards achieving a zero carbon emissions by 2050 and advocated a 55 % reduction of emissions by 2030 [1].

Like any ambitious project, Europe's fundamental transformation to "green" demands radical changes and breakthrough technologies. Renewable energy sources like solar cells and wind-power stations are already well-established and successfully functioning around the world. Batteries, especially Lithium ion batteries, are nowadays the undeniable choice for powering small portable devices and even vehicles. In recent years, however, fuel cells (FCs) are recognized as a promising additional option for the above-outlined challenge. Multiple fuel cells are now existing, which are classified on the type of fuel used and the type of electrolyte composing their architecture such as: molten carbonate fuel cells (MCFC), solid oxide fuel cells (SOFC), direct methanol fuel cells (DMFC), alkaline fuel cells (AFC), phosphoric acid fuel cells (PAFC), proton-exchange membrane fuel cells (PEMFC) and anion exchange membrane fuel cells (AEMFC). Nonetheless, among those, hydrogen-fueled proton-exchange membrane fuel cells (PEMFCs) are the most promising and flexible option due to their environmental sustainability, high energy density, high energy-conversion efficiency and low operating temperatures [2]. Hydrogen fuel cells have a very high efficiency of ~65%. For comparison: the efficiency of the best combustion engines is around 35-40%. For solar power plants, it is only about 15-20% and is highly dependent on weather conditions. The wind power plant's efficiency reaches 40%, but wind turbines also require suitable weather conditions and expensive maintenance. Moreover, the abovementioned Green Deal identified hydrogen as a priority area. Hydrogen is increasingly seen as the key element that will serve as the main energy carrier when fossil fuels will be completely abandoned, and renewable energy sources will not be able to meet the required needs. Due to these numerous benefits, PEMFCs are expected to become a mainstream power source for a wide range of devices, ranging from stationary and portable [3] electronics to vehicles [4], eventually becoming one of the pillars of a future sustainable green-energy system.

1.2. Proton-exchange membrane fuel cells

A PEMFC is an electrochemical cell that functions through converting the chemical energy of hydrogen into the electrical energy, with zero harmful emissions since it generates only pure water and heat as by-products. A membrane electrode assembly (MEA) is at the core of a PEMFC and is the most important component. It contains anode and cathode compartments separated by a special proton-conducting and, at the same time, electrically insulating polymer electrolyte membrane, as shown in the simplified schematic in Figure 1. H_2 and O_2 (or air) gases are supplied to opposing electrodes through the micro-porous gas diffusion layers (GDL) and flow fields. At the anode side, the hydrogen oxidation reaction (HOR) occurs where hydrogen splits into protons and electrons. The resulting protons migrate through a polymer membrane (typically Nafion) to the cathode. At the same time, electrons, which cannot pass through the membrane, run through an electrical circuit to produce electric power. On the cathode side, the oxygen reduction reaction (ORR) takes place: protons, passed through the membrane, and electrons, returned from doing work, recombine with the oxygen supplied to the cathode to produce water as its only emission. The overall cell reaction is:

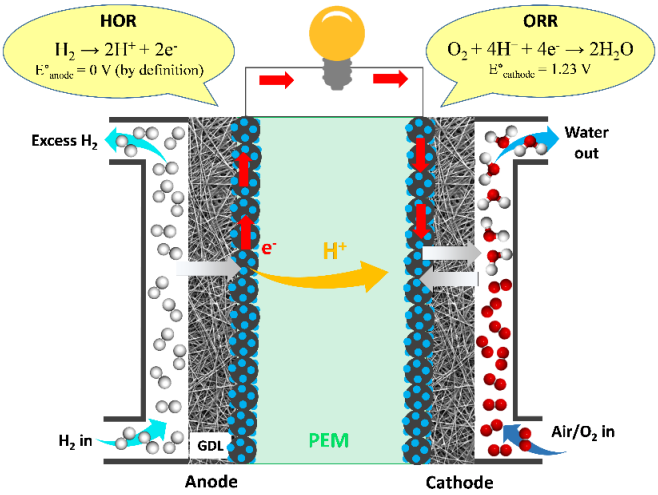

Figure 1. A simplified schematic illustration of a single cell membrane electrode assembly.

$$2H_2 + O_2 \rightarrow 2H_2O \qquad E^\circ_{cell} = 1.23 \text{ V}$$

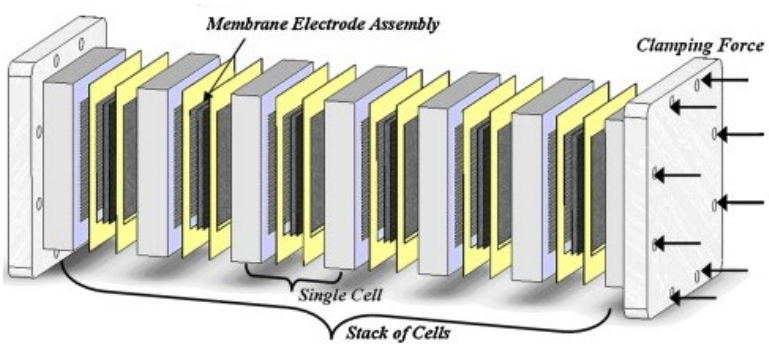

Figure 2. Schematic illustration of the PEMFC stack. Reproduced from [5], Copyright 2009, with permission from Elsevier.

Due to the relatively low voltage produced by a single cell, the cells are usually combined into a so-called fuel cell stack with an acceptable output voltage and current for specific application (see Figure 2). A typical fuel cell stuck can be composed even of hundreds of individual cells.

2. State of the art

2.1. Proton-exchange membrane fuel cells: Current status and challenges

Nowadays, PEMFCs are being intensively developed and their commercialization is dawning. Thanks to their modular structure, fuel cells can be utilized in a broad number of applications ranging from massive stationary power plants to compact portable power units. PEMFCs for stationary applications are being used extensively for commercial, industrial, and even residential purposes due to multiple advantages over conventional fossil fuel plants such as high efficiency, zero emissions, reduced noise production, and requirement of less space. It is a primary power source to power buildings that are not connected to the grid or to provide supplemented power. With their ability to scale from singular units to megawatt-scale establishments, they are capable to power a wide range of facilities, from smaller family houses to residential applications, stores, buildings, and larger structures in the commercial sphere, and even data centers and power plants in the industrial sector. Generally, stationary fuel cells are divided into three types:

- Combine heat and power (CHP) – except of electricity it uses the heat generated by fuel cell, which can be further used to heat water or provide space heating for buildings.
- Uninterruptable power supply (UPS) – produce uninterrupted power and used as backup power in critical facilities like hospitals or server farms.
- Primary power units – large stationary units used to generate power for facilities or for the grid.

The Ballard Generation Systems, with its 250 kW output power, is the largest power plant to date [6]. It can produce enough electricity for a small apartment complex or commercial building, or about 50 family houses.

The ability to maintain efficiency while their size is reduced makes PEMFCs suitable for operating as small power generators. Portable fuel cell systems can effectively substitute batteries in many compact/mobile applications like laptops, cellular phones, military radio/communication devices, battery chargers, unattended sensors, etc. [3]. The power of portable fuel cells usually ranges from 5 to 50 W [7]. Nevertheless, the portable power has the

smallest share within the fuel cell market due to the competitiveness and performance improvement of battery technology.

Among many applications of PEMFCs, the transportation sector is the most competitive and promising [6,8]. Major motor brands have been extensively developing PEM fuel cell technology producing FC cars, FC buses, heavy-duty vehicles, and even trains [9]. A major milestone for PEMFC commercialization in the transportation sector was introducing the first commercial Mirai hydrogen fuel cell vehicle (HFCV) by Toyota in 2014. Nowadays, three HFCVs are available in the market: Hyundai NEXO [10], Toyota Mirai [11], and Honda Clarity [12]. The comparison of their FC power and driving range is shown in Table 1. Moreover, several dozen urban transit fuel cell buses are operating in cities worldwide, although they are not yet in series production. In September 2018 Alstom company equipped German railways with the first hydrogen trains [13,14]. Hydrogen-powered trains are also expected to enter the British railway network from 2022 [15]. Fuel cells are currently also under studying to be employed in aviation for powering drones or unmanned aerial vehicles [16]. Moreover, aviation giant Airbus announced ZEROe concept aircraft, which is expected to use hydrogen fuel cells to create electrical power that complements the modified gas-turbine engines, resulting in a highly efficient hybrid-electric propulsion system [17]. Overall, the power output for the automotive fuel cell ranges from ~100 to 200 kW or more.

	Hyundai Nexo	Honda Clarity	Toyota Mirai
Stack Max. Power (kW)	95	103 kW	114 kW
Range (km)	610	590 km	500 km

Table 1. HFCV power and driving range. Data adopted from [7].

Due to the numerous benefits of fuel cells across multiple sectors, the global investment together with the green energy initiative, the hydrogen fuel cell market is expected to witness a phenomenal growth in the near future.

Despite dawning commercialization and great potential, such fuel cells are not without problems to solve. Large-scale deployment of PEMFCs has been hampered due to several shortcomings. Alongside more general ones being the hydrogen production and the underdeveloped hydrogen infrastructure, relatively high costs and limited lifetime of PEMFCs are the two major barriers that still exist. Both are currently under the considerable focus of researchers.

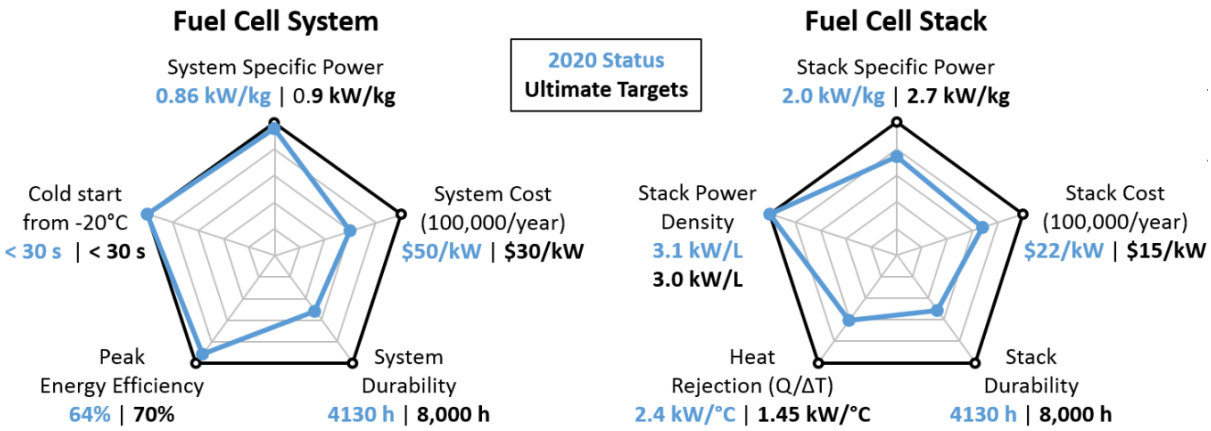

Figure 3. Diagrams illustrating current status of automotive fuel cell systems (left) and stacks (right) relative to ultimate subprogram targets in key areas. Adopted from ref. [18].

To ensure PEMFCs' competitiveness, the US Department of Energy (DOE) set multiple targets for a fuel cell system. Figure 3 illustrates the diagram comparing the current status of automotive fuel cell systems and stacks with the ultimate targets in key areas [18]. The diagrams reveal that additional research and development efforts should be performed to improve fuel cell cost and durability in order to meet all targets for fuel cell systems.

The catalytic layer plays a pivotal role in such fuel cells facilitating reactions on both electrodes. Among all components, the catalytic layer alone represents a major part of the fuel cell's total costs and it is not reduced even by scaling up production, as shown in Figure 4 [19]. So far, platinum remains the only choice that meets catalysis requirements for both HOR and ORR [20]. Current commercial PEM fuel cell catalyst typically consists of highly dispersed Pt nanoparticles dispersed on carbon black. However, platinum is expensive and rare. Furthermore, high Pt loading of about 0.3 mg_{Pt} cm^{-2} is required to reach the target lifetime without major efficiency loss. For example, total Pt loading in commercial Toyota Mirai FCV is 0.365 g cm^{-2} (anode loading of 0.05 g cm^{-2} and cathode of 0.315 g cm^{-2}) [8]. It should also be kept in mind that the abundance of platinum, coupled with an expected increase in demand if the industry eventually shifts to fuel cells, are likely to affect its availability and price for the worse. The reduction of platinum content has been thus the primary approach for reducing the PEMFC costs.

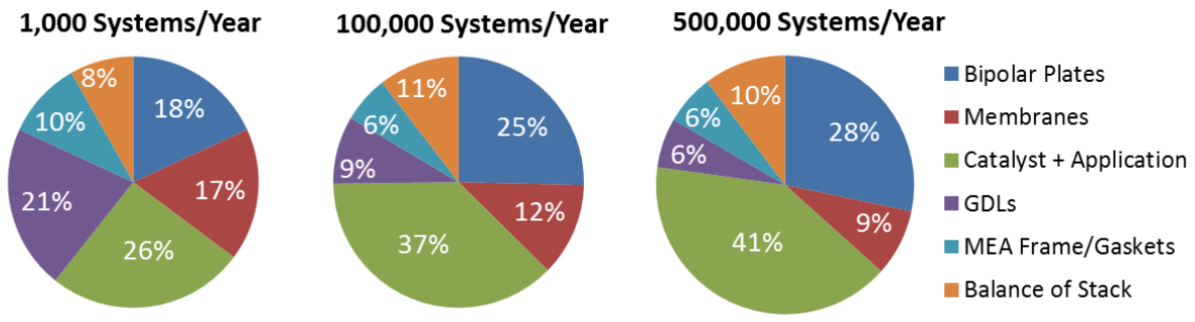

Figure 4. Breakdown of the 2017 projected fuel cell stack cost at 1,000, 100,000, and 500,000 systems per year. Adopted from ref [19].

The DOE developed the special technical targets for the catalytic layer itself to evaluate progress without testing entire systems. The total amount of Pt at both electrodes has been set to be less than 0.125 g cm^{-2} by 2025 [19]. This has triggered intensive research to seek approaches to reduce Pt loading in fuel cell.

In recent years extensive research and development has allowed to significantly decrease Pt loading on the anode side down to 0.05 mg_{Pt} cm^{-2} without substantially influencing the cell performance. Yet, reducing cathode loadings still remains a challenge. The cathode four-electron multistep ORR is six or even more orders of magnitude slower than the anode one-electron HOR and consumes most of the catalyst material requiring approximately 10-times higher catalyst loading than the anode [21]. A decrease in cathode catalyst loadings usually strongly affects fuel cell activity and stability. Consequently, the requirements for ORR catalysts are very rigorous. Based on the foregoing, recent academic and industrial research efforts are addressed to accelerate the ORR and, at the same time, minimize the quantities of platinum at the cathode to meet the abovementioned cost-performance requirements.

Apart from cost-efficiency, catalyst durability is another significant drawback that certainly deserves attention. The lifetime of a fuel cell is always associated with degradation processes occurring at electrodes, especially the cathode. Catalyst/support assemblies are exposed to corrosive environment of the fuel cell cathode during its operation facing low pH and relatively high potentials (from 0 to 1.5 V) [22]. The severity in operating conditions is further exacerbated by the transient and cyclic nature of the PEMFC operating conditions, especially for automotive applications. For example, at load cycle operation of a PEMFC potential on the cathode is below 1.0 V versus the reversible hydrogen electrode (V_{RHE}), and at the start/stop of the device, potentials can reach as high as 1.5 V_{RHE} due to the simultaneous presence of oxygen (air) and hydrogen in the anode compartment. Such conditions always occur during the purging

of the anode compartment with hydrogen at start-up or with air at shut-down and were found to be the most harmful to both catalyst and its carbon supports, initiating a decrease of the electrochemically active surface area (ECSA).

The activity of fuel cell catalyst should be maintained over an extended period of fuel cell operation. According to the DOE, the lifetime target is from 5,000 to 80,000 operating hours depending on the specific application (5,000 for portable, 8,000 for automotive, and 60,000-80,000 for stationary fuel cell systems) [19]. The durability and reliability of catalyst may thus pose even greater obstacle than its cost-efficiency for PEMFCs fast and sustained market penetration, especially for automotive applications [20]. Up to now, promising results were achieved by Toyota Mirai, which passed the 3,000 operating hours in the real world, which is still far from the aforementioned standards [8].

However, it is impractical, if not impossible, to test every fuel cell for 8000 hours. Moreover, the complexity of the multicomponent PEMFC system further complicates such types of investigations. That is why special accelerated stress tests (ASTs) protocols were developed. They allow accurately simulate degradation of a whole cell or a particular component within the MEA of a PEMFC in a practical timeframe and obtain reliable information about their degradation, thus elucidating fundamental phenomena undetectable in complex systems. In particular, AST protocols allow testing specifically the durability of the fuel cell catalyst. It consists of 30,000 triangular potential sweep cycles from 0.6 V_{RHE} to 1.0 V_{RHE} at 50 mV/s sweep rate [23]. This test takes about 130 h, which is much faster than the required 8,000 h for automotive applications. Furthermore, ASTs were developed to test catalyst support stability. It differs from the latter one and consists of 5,000 triangular potential sweep cycles from 1.0 V_{RHE} to 1.5 V_{RHE} at 500 mV/s sweep rate [23]. Lower than 40% loss of initial catalysts mass activity and surface area during both ASTs has been set as a target for catalyst stability. ASTs can be performed on real PEMFC systems (*in situ*) or using an electrochemical cell with liquid electrolyte mimicking the membrane (*ex situ*). The advantage of *ex situ* ASTs is that they allow better control of the degradation conditions and thus can predict the fuel cell's lifetime while saving the material costs required for in situ testing in real fuel cells.

Up to date, several closely related general degradation mechanisms have been identified for platinum and platinum-based cathode catalyst. They are divided into two classes: primary and secondary and are illustrated in Figure 5. Primary degradation mechanisms include carbon (support) corrosion and platinum dissolution [24,25]. Carbon corrosion induces secondary degradation mechanisms like platinum particle detachment or agglomeration. The secondary

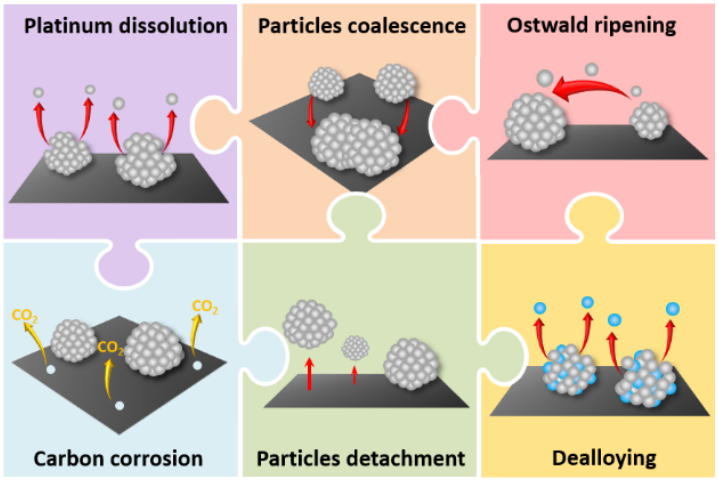

Figure 5. Simplified representation of degradation mechanisms for cathode catalyst on a carbon support in fuel cells.

degradation mechanisms associated with platinum dissolution are Ostwald ripening and Pt redeposition into a membrane [26,27].

Platinum is known to be thermodynamically stable element but according to the Pourbaix diagram it is dissolving at potentials higher than about 0.9 V_{RHE} at pH values lower than two, which are typical for PEMFC cathode environment. The dissolution of Pt was detected using an electrochemical scanning flow cell (SFC) with online detection by inductively coupled plasma mass spectrometry (ICP-MS) for a wide range of potentials, pH and types of catalysts [28,29]. The dissolved Pt can accumulate in the membrane influencing its operation [27]. Moreover, it can redeposit back to the catalytic layer but on larger nanoparticles. The later effect is known as Ostwald ripening when large particles grow at the expense of smaller ones due to differences in surface energy [27,30] leading to Pt catalyst coarsening and concomitant decreasing of its surface area.

Carbon is also sensitive to conditions relevant to fuel cell operation [31]. The carbon oxidation (corrosion) reaction is very slow but can be enhanced at higher potentials representing start–stop cycles. The corrosion of the support in the vicinity of platinum particles weakens their bonding, which leads to particle movement with further coalescence or even particles detachment [32,33]. Moreover, in the case of alloys of platinum, faster leaching of less noble metals influences all the above mentioned processes [25].

2.2. Recent strategies for the development of cost-efficient cathode catalysts

2.2.1. PGM-free cathode catalysts for PEMFCs

Several novel strategies have been put forth by the researchers towards reaching higher cost-efficiency of ORR catalysts. Among all, the most intriguing, yet the most challenging approach is replacing Pt with non-precious metals (so-called platinum group metal (PGM)-free catalysts). Indeed, recently many PGM-free ORR catalysts have been extensively investigated and have been shown potential to be considered as cathode catalysts in PEMFCs.

In a last decade, significant progress has been made in PGM-free catalyst development. Among them, the M-N-C catalysts containing nitrogen and transition metal-doped carbons (M: Fe, Co, Mn), represent the most promising ORR catalysts for PEM fuel cells [34–37]. To replace platinum-based catalysts for ORR, PGM-free catalysts must show activity at least 1/10 of Pt-based catalysts i.e. >0.044 A/cm^2 at 0.9 V_{RHE} [19], excellent mass-transport properties, and high durability. Despite exhaustive research in nonprecious metal and even metal-free ORR catalysts have not yet shown sufficient power density owing to poor mass-transport properties. This is because of relatively high PGM-free catalyst loading at the cathode of the MEAs (3.8 and 4.1 mg cm^{-2}) which is needed to compensate their lower activity [34,35]. Challenges also remain to maintain the electrochemical performance and durability of catalytic materials at the PEMFC cathode [37,38]. A significant effort is further needed to achieve full understanding of PGM-free catalyst instability and to derive correlations between stability and intrinsic materials properties. A catalyst completely free of platinum seems to be an ideal solution, but limited performance of this type of catalysts and their poor stability hinder their commercial availability for the fuel cell industry, at least in the near future.

2.2.2. Shape-controlled platinum cathode catalysts for PEMFCs

Tuning the geometry/dimension of pure platinum represents another effective strategy on the way to conceiving a new cathode catalyst. It allows increasing as much as possible the active surface of the catalyst and can be realized by the preparation of high surface-to-volume ratio of the Pt catalyst through the development of three-dimensional Pt architectures or shape-controlled Pt nanoparticles with selectively exposed facets. In this regard, multi-shaped Pt nanoparticles such as concave cubic [39,40], hexagonal [41], tetrahedral-octahedral [41] and high-index tetra-hexahedrons [42,43] together with various Pt nanostructures like nanowires (NWs) [44–48], nanorods [49–51], nanotubes [52,53] and hollow structures [54,55] have been synthesized and tested for ORR activity. Among them ultrafine jagged platinum nanowires NWs (J-PtNWs) deserves particular attention. Due to their highly stressed, undercoordinated rhombus-rich surface configuration J-PtNWs showed very high specific activity (SA) of 10.95 mA cm_{Pt}^{-2}, unprecedentedly high mass activity (MA) of 13.6 mA mg_{Pt}^{-1} at 0.9 V_{RHE} and enhanced stability [47]. Although such strategy leads to better Pt utilization efficiency, it cannot increase the ORR kinetics itself. Furthermore, complex and expensive fabrication process make this strategy not completely suitable for the desired goal.

2.2.3. Platinum-based bimetallic alloy cathode catalysts for PEMFCs

In order to increase the ORR kinetics, the mechanism of the reaction has to be taken into account. The understanding of the ORR catalytic activity falls under the Sabatier-volcano principle of heterogeneous catalysis representing the catalyst activity towards ORR (logarithm of the exchange current density) as a function of oxygen and OH adsorption energy (ΔE_O, ΔE_{OH}) as shown Figures 6a and b. As the reaction intermediates, O and OH adsorption energy thus serves as a valid activity descriptor for ORR catalysts. Such volcano-like plots are commonly used to estimate how close the catalyst is to the optimum performance for a given reaction. For example, for elements that bind oxygen too strongly (left side of the volcano in Figure 6a), the reaction rate is limited because the catalyst surface is strongly oxidized (poisoned by reaction intermediates). And vice versa, for elements that bind oxygen too weakly (right side of the volcano), the ORR rate is limited by the dissociation of O_2. Extrapolation of these two trends towards increasing exchange current density leads to the peak of the volcano. Platinum appears to be the closest element to the theoretically predicted peak (red line in Figure 6a) for ORR as compared to many other elements. However, the graph also hints that platinum still bind oxygen too strongly to be optimal. Consequently, there is a space to improve cathode catalyst activity by decreasing intermediate binding energies by about 0.2 eV. This can be realized by the precise engineering of platinum catalyst through tuning its electronic structure, the Pt-Pt interatomic distance, and the coordination number [56–58].

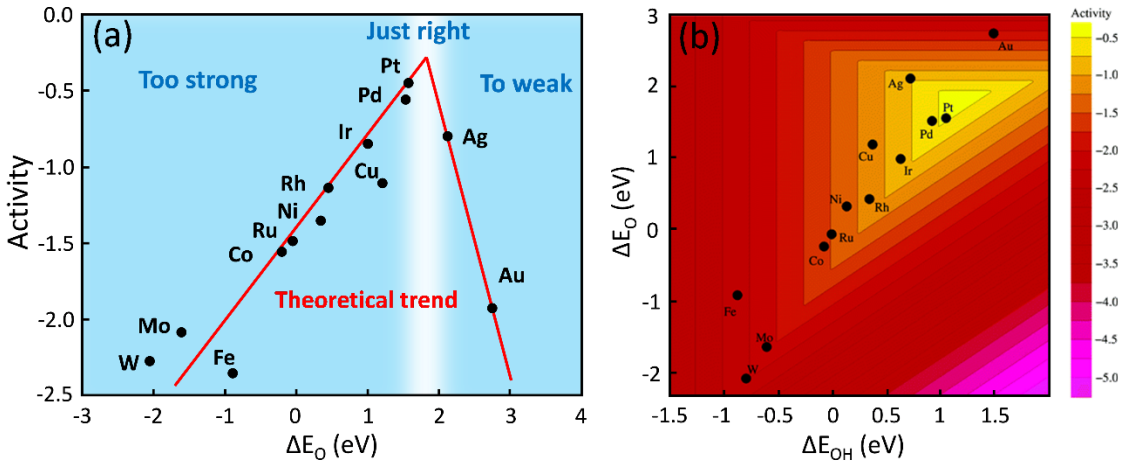

Figure 6. Volcano plots for the oxygen reduction reaction: (a) Trends in oxygen reduction activity of different elements plotted as a function of the oxygen binding energy; (b) Trends in oxygen reduction activity plotted as a function of both the O and the OH binding energy. Reproduced with permission from [21], Copyright 2004, American Chemical Society.

One of the most promising ways to do that is to add the selected element to platinum, i.e., to produce a Pt-based alloy [59]. Alloying of platinum represents the third and the most promising strategy nowadays to increase the cost-efficiency of the ORR catalyst. The development of efficient and robust Pt-based bimetallic catalysts relies on a fundamental understanding of the structure-activity-stability relationship. That is why extensive experimental and theoretical studies were primarily focused on extended surfaces of Pt-alloys (including two-dimensional single-crystalline or polycrystalline bulk and thin-film (TF) surfaces) allowing control at the atomic level. This approach minimizes the complexity of a real technological catalytic system but, at the same time, maintains its essential properties. Catalytic studies on such systems have revolutionized the understanding of catalysis over bimetallic surfaces by providing detailed insight into the underlying surface chemistry. An enhancement of the ORR activity in comparison to pure platinum has been demonstrated for a wide range of platinum alloys with rare-Earth metals (REM), 3d-transition metals (3d-TM), and lanthanide metals.

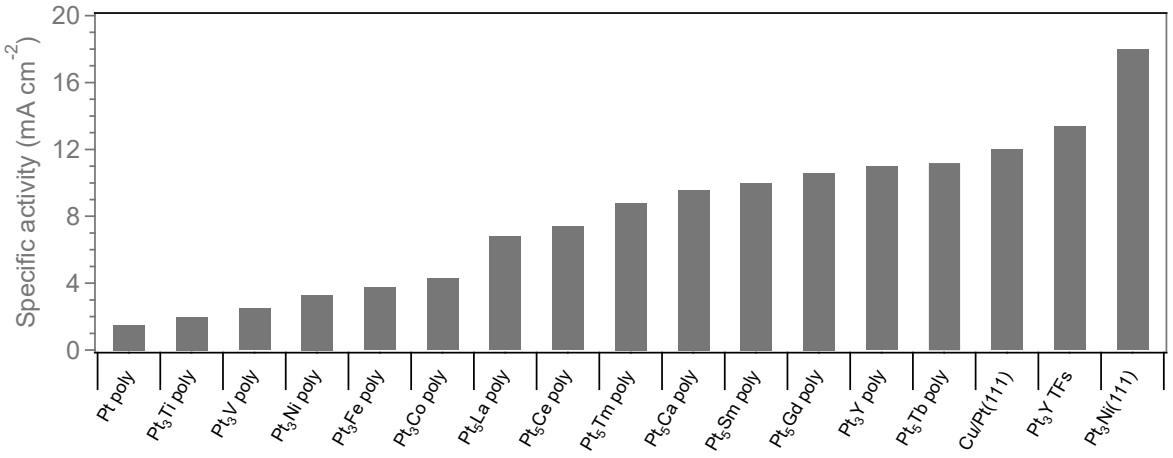

Figure 7. Summary of surface specific activities for the most active Pt-based extended electrode surfaces obtained from rotating disk electrode (RDE) measurements in the half-cell in acidic electrolytes at 0.90 V_{RHE}. Data obtained from refs. [58–62].

Figure 7 summarizes a comparison of the real surface area-based activity (denoted as specific activity, SA) for the selection of the most active Pt-based extended surfaces obtained from a rotating disk electrode (RDE) measurements in the half cell in acidic electrolyte. Stamenkovic et al. provided experiments on extended polycrystalline surfaces and showed that among Pt-based 3d-TMs Pt_3Co had the highest ORR activity, followed by Pt_3Fe, Pt_3Ni, Pt_3V, and Pt_3Ti, respectively (Figure 7) [58]. In addition to 3d-TMs, polycrystalline platinum alloys with lanthanides and REM elements were identified as promising alloying elements to enhance

the ORR activity. Pt_5La, Pt_5Ce, Pt_5Tm, Pt_5Ca, Pt_5Sm, Pt_5Gd, Pt_5Tb, and Pt_3Y alloys showed an enhancement in SA by a factor of 3 to 10 over polycrystalline Pt [59–61]. The PtNi alloys were further investigated by Stamenkovic *et al*. using a model single-crystal surfaces. They developed a special Pt-skin $Pt_3Ni(111)$ surface structure showing improved ORR activity by a factor of 10 with respect to the Pt(111) surface which was a direct proof of the alloying effect. Subsequent studies on model single-crystal surfaces showed that incorporating submonolayer quantities of Cu into Pt(111) resulted in an 8-fold improvement in oxygen reduction activity [63]. It has been shown that a so-called Pt-skin surface is formed during the initial acid treatment. The structural and electronic effects of alloying metals in the subsurface play a significant role in weakening the adsorption of oxygen containing species.

Figure 8a represents the Sabatier-volcano plot for some selected Pt-based alloy catalysts (now data are shown relative to pure platinum). The plot demonstrates that many bimetallic systems show slightly weaker bonds to oxygen than the pure Pt and show superior ORR activity. Furthermore, the partial replacement of platinum by cheaper and more abundant element (see Figure 8b) lowers the overall cost of the catalyst.

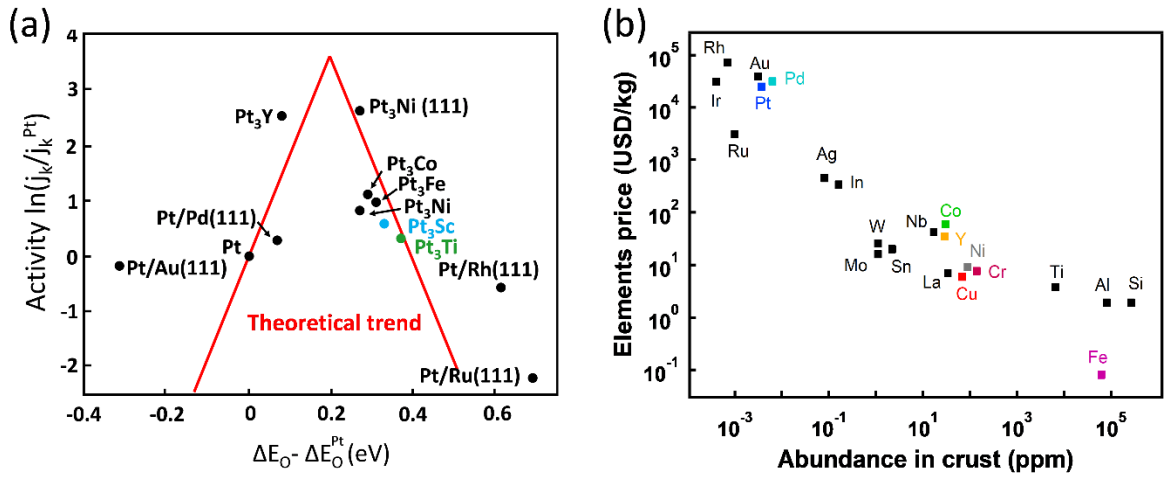

Figure 8. (a) Measured kinetic current density for a range of Pt-based alloy catalysts plotted as a function of the oxygen binding energy (data are shown relative to Pt). The red lines represent the theoretical predictions. Reproduced with permission from [59]*, Copyright 2009, Nature Publishing Group; (b) Price of the elements versus their abundance in the Earth crust.*

The d-band theory established by Nørskov and Hammer back in the 1990s linking the surface adsorption strength with the different d-band filling of the metal was used for the explanation of the bimetallic catalyst structure-activity relationship [64,65]. An upshift of d-band center (E_d) in bimetallic alloys compared to monometallic platinum catalysts was claimed to be responsible for decreasing the adsorption energies of reaction intermediates and thus

increasing ORR activity. Such shift was attributed to two main effects illustrated in Figure 9, namely electronic (ligand) and geometrical (strain). The ligand effect in a bimetallic system is caused by the modification of the d-states of the surface Pt atoms given by electronic charge transfer between Pt and alloying metal. In turn, the geometrical effect refers to the different ionic radii of the alloying atoms, which induces a lateral compressive arrangement of Pt atoms on the surface (surface strain Both bring beneficial effects on weakening of the binding energy of reaction intermediates.

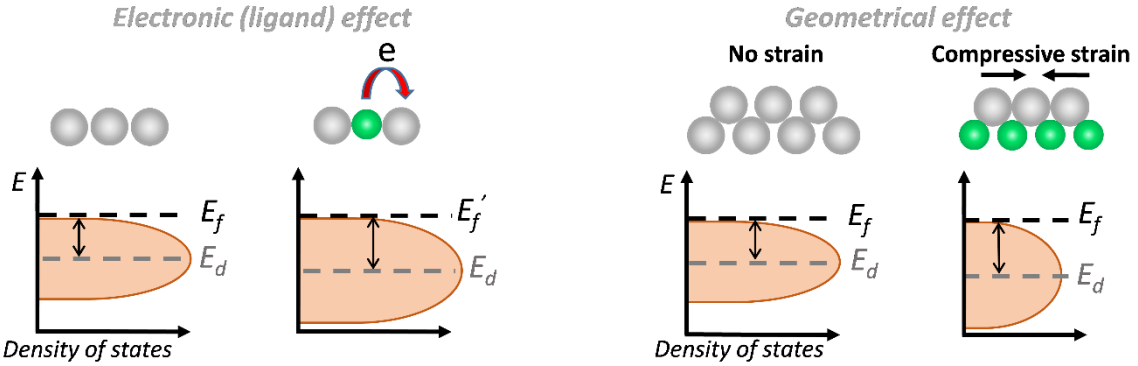

Figure 9. Schematic illustrations of ligand and strain effect caused by alloying on the electronic structure of platinum.

The aforementioned studies have produced invaluable knowledge that has been used for the ORR catalysts preparation up to now. The application of the knowledge obtained from studies on Pt-based extended surfaces enabled the development of bimetallic nanoparticles for ORR. Figure 10 shows a comparison of the specific activity and Pt-mass normalized ORR activity (denoted as mass activity, MA) obtained from rotating disk electrode (RDE) measurements in the half cell in acidic electrolyte for the selection of some of the most active ORR electrocatalysts. The red line indicates the DOE 2020 technical target for MA of ORR catalysts [19]. Stamenkovic *et al*. produced highly uniform Pt_3M (M = Ni, Co, Fe) nanoparticles prepared by an organic solvothermal method supported on high surface area carbon with activity improvement factors of 2-3 versus conventional Pt/carbon catalysts [66,67]. Li *et al*. demonstrated well-designed core/shell structured $L1_0$-CoPt/Pt NPs with a tetragonal intermetallic hard-magnet CoPt core and a 2-atom-thick Pt shell. The $L1_0$-CoPt/Pt NPs showed superior ORR activity in the liquid half-cell test with SA and MA being ~38 and ~19 times higher than those measured on Pt/C [68]. Hernandez-Fernandez *et al*. in turn, reported highly active mass-selected Pt_xY NPs with mass activity of up to 3.05 A mg_{Pt}^{-1} prepared through the

gas-aggregation technique [69]. Even higher MA of 3.6 A mg_{Pt}^{-1} was reported for mass-selected Pt_xGa NPs prepared using the same technique by Velázquez-Palenzuela *et al*. [70].

The combination of composition control and precise surface engineering has led to even further increase in the specific and mass activities of the ORR catalysts. In a past decade, bimetallic octahedral nanoparticles [71–73], nanoframes [74], nanowires [75–77], nanopalets [78], etc. were synthesized and showed MA which largely exceeds the commercial Pt/C and the DOE target of 0.44 A/mg_{Pt} [19]. Among them, Mo-doped PtNi nano-octahedra showed ~80- and ~70-fold enhancements in specific and mass activity for ORR, respectively, compared with commercial Pt/C catalysts [73]. Yet the record MA so far belongs to self-supported Pt-CoO networks and Pt_3Co alloy supported over PGM-free materials (denoted as LP@PF) showing 8.4 and 12.4 A mg_{Pt}^{-1}, respectively [79,80].

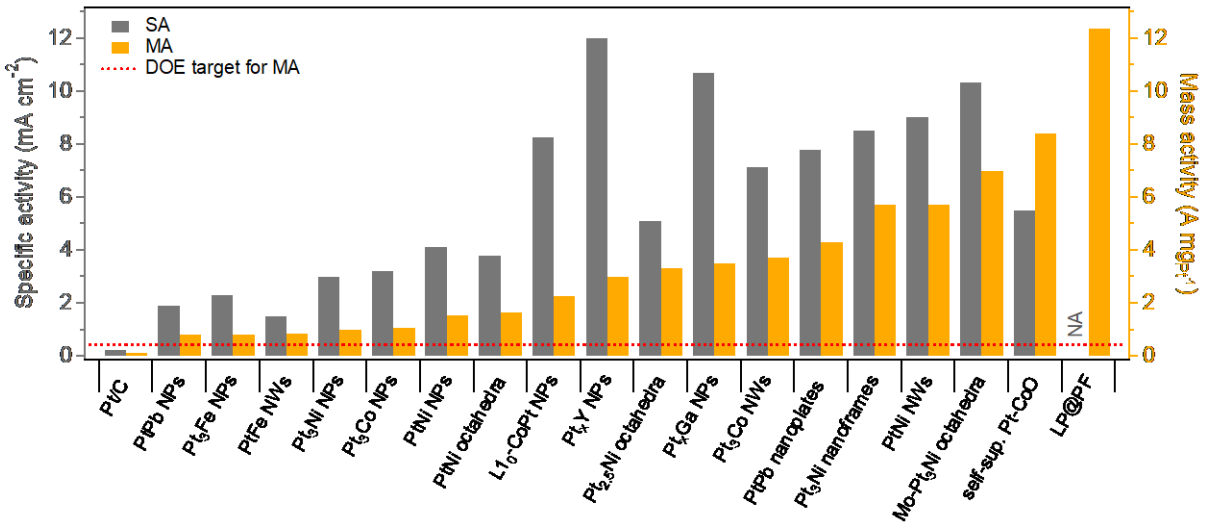

Figure 10. Summary of specific (left axis, grey bars) and mass (right axis, orange bars) activities the most active ORR electrocatalysts obtained from rotating disk electrode (RDE) measurements in the half-cell in acidic electrolytes at 0.90 V_{RHE}. NA stands for not available value. Data obtained from refs. [66–80].

Bimetallic catalysts are nowadays at different stages of research and development. Some of them have successfully entered the market, such as Pt-Co nanoparticles which are used in the Toyota Mirai fuel cell vehicle [81] while some were investigated only in well-defined half-cell conditions using RDE measurements but have not been even investigated in real fuel cells. As technology has now started reaching performance targets, the long-term stability of Pt-based catalyst as a second drawback for PEMFCs commercialization has become the most important challenge to be addressed.

2.3. Investigation of catalyst degradation mechanisms

Bimetallic catalysts are very complex systems, where both structure and composition dynamically change under specific reaction conditions. The reactive gases, temperature as well as pressure conditions of catalytic reactions can initiate interdiffusion of constituent elements and significantly affect valuable properties of alloy materials [82–85]. The catalyst thus "adapts" to the reaction medium. Such behavior is a complex phenomenon driven by the interplay of multiple parameters, such as bonding of each metallic component with a given adsorbate, their surface energies, diffusion barriers, etc. Moreover, in the case of fuel cells, potentials on the cathode and low pH environment could further complicate alloy behavior and must be taken into account. For example, during high load operation of the fuel cell (0.6-0.8 V) the catalyst is in its metallic state. Contrary, during shut-down or start-up conditions (potential is 0.95-1 V and up to 1.5 V, respectively) the cathode catalyst is oxidized. The thermodynamic stability of the metal M, as a rule, much lower than that of platinum [25] resulting in selective dissolution of M in the acidic environment during fuel cell operation. Monitoring the dynamic behaviour of bimetallic catalysts under specific reaction conditions thus poses greater challenges and is of utmost importance in order to advance the understanding of the alloy restructuring at real conditions for the knowledge-based development of highly effective and stable cathode catalysts in the future.

Although fuel cell catalyst stability has been studied for a long time it was performed mainly *ex situ* by providing ASTs in electrochemical cell and characterization of a catalyst surface before and after stability tests with conventional surface science spectroscopic and microscopic tools. This led to a rather superficial knowledge about true environment-induced changes of catalysts in the course of electrochemical reaction [86]. That is why additional progress in catalyst characterization was highly demanded in order to provide in-depth insights into catalyst behavior directly at the electrified solid-liquid interface i.e., to perform so-called *in situ*/*in operando* measurements [86–88]. By definition, "*in situ*" describes characterization of the catalyst under conditions relevant or identical to the catalytic operation. In turn, "*in operando*" combines *in situ* characterization of the working catalyst during the actual reaction with simultaneous measurement of its catalytic activity [89]. Reaching such goals certainly require multisectorial and multidisciplinary approaches where electrochemistry is combined with material science and surface science.

A precise examination of surface chemistry underlying the ORR mechanism and catalyst degradation has been very limited due to experimental difficulties. Due to the complex architecture of PEMFC device *in situ/in operando* characterizations of cathode catalysts inside the real cell are still rare. They are mostly based on using high-energy X-rays at synchrotron facilities that are able to penetrate through the cell. Nowadays, much effort has been directed on adapting existing traditional surface science analytical methods, which generally operate under ultrahigh vacuum (UHV) conditions, to pass the pressure gap to be able to probe a catalyst exposed to high pressures or even liquids. Various powerful microscopic and spectroscopic methods have been recently developed to characterize catalyst structure, morphology, composition, and chemical state directly at electrified solid-liquid interface inside specially designed electrochemical cells under well-defined half-cell conditions, which become necessary for elucidating fundamental phenomena undetectable in complex systems. The most common *in situ/in operando* techniques are schematically summarized in Figure 11.

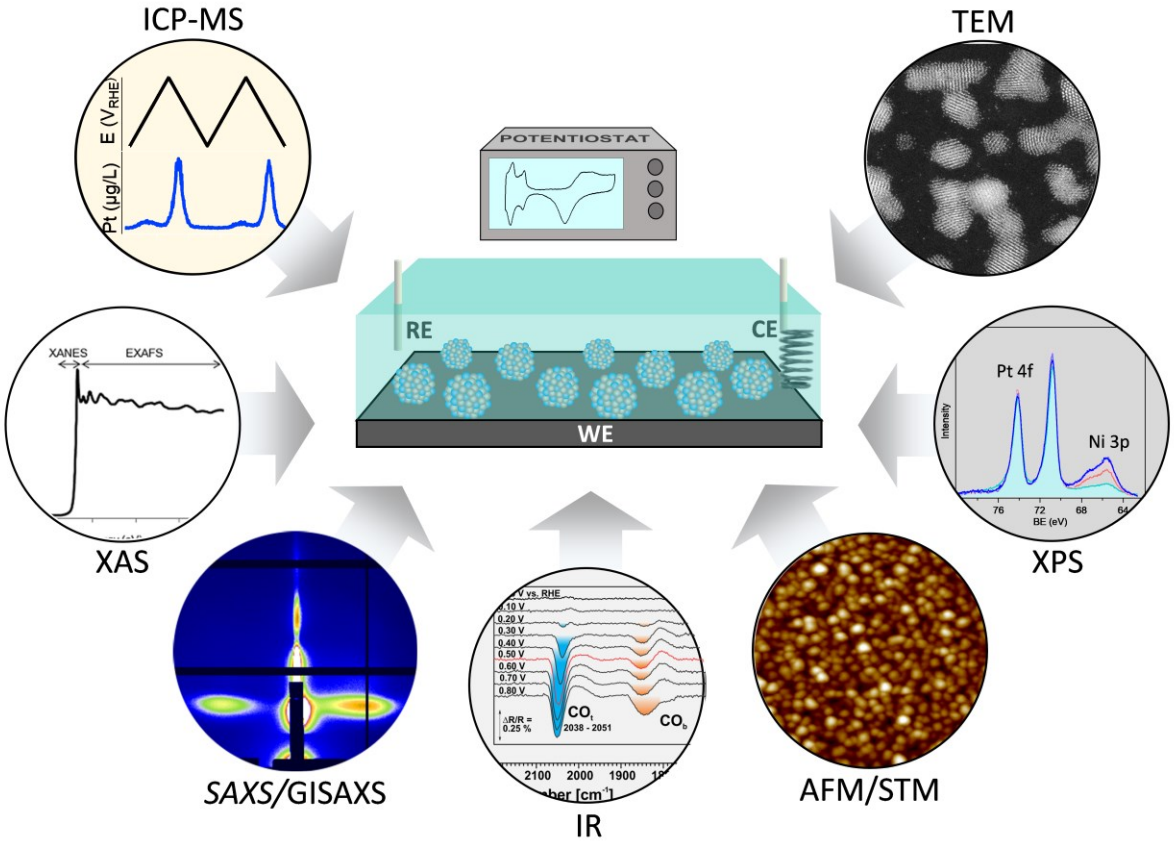

Figure 11. Schematic representation of the selection of in situ/in operando characterization techniques used to investigate the cathode catalyst degradation in PEMFCs.

Electrochemical cells involved in these *in situ/in operando* measurements differ from technique to technique and from experiment to experiment in their structure, shape, volume, etc. However, mostly all of them have the three-electrode configuration containing the reference electrode (RE) to provide a reference point for voltage, the counter electrode (CE) to close an electrical circuit and measure current, and the working electrode (WE) representing the investigated sample. The PEMFCs working environment is simulated inside those cells in a low concentrated acidic electrolyte (mimicking the Nafion membrane) by potential variations using both potentiostatic and/or potentiodynamic (cycling) modes.

Advances in design and construction of electrochemical cells have significantly increased the possibilities of the state-of-the-art techniques, and the degradation of the fuel cell catalyst has received renewed boosted interest and is becoming a spotlight for researchers. Studies using atomic force microscopy (AFM) [90,91], scanning tunneling microscopy (STM) [92–94] and transmission electron microscopy (TEM) [95,96] are extensively used to investigate morphological changes of Pt and Pt-based catalysts under conditions resembling a working fuel cell and directly interconnect obtained results with ECSA calculated from simultaneously recorded cyclic voltammograms, thereby significantly contributing to understanding the relationship between morphology and performance of catalysts.

Recently, *in situ/in operando* X-ray scattering methods have become popular as a complement (or substituent) to *in situ* microscopy techniques because they are able to probe in-depth mean structure variation in a catalyst structure by analyzing a larger sample area in a relatively short time and provide very good statistical accuracy. In this framework, small angle X-ray scattering (SAXS) proved to be a suitable method. SAXS can be carried out in transmission or at grazing incidence conditions (GISAXS). Up to now, it was shown that electrochemical-based SAXS analysis can be used to study catalyst degradation in an electrochemical environment [97–99]. More recently electrochemical-based GISAXS was applied to investigate the roughening of the Pt(111) single-crystal surface during electrochemical cycling [93].

In addition to online information about catalyst morphology, many specially designed *in situ* spectroscopic techniques are used to investigate its electronic structure and chemical composition. Synchrotron X-ray-based spectroscopy is the most common for that due to the ability of X-rays to penetrate into electrochemical setup. For example X-ray absorption spectroscopy (XAS) developed rapidly and became the most popular tool for investigating the catalyst *in situ/in operando* under electrochemical conditions. XAS includes both X-ray absorption near-edge spectroscopy (XANES) spectroscopy, which gives the information about

oxidation states of the catalyst, and extended X-ray absorption fine structure (EXAFS) spectroscopy which, in turn, probes interatomic distances and coordination number [100–102]. X-ray photoelectron spectroscopy (XPS) is another exceptionally powerful tool for high-resolution characterization of the catalyst elemental composition and electronic structure. It can be used to identify elements in the alloy and their oxidation states, estimate their relative concentration, charge transfer due to alloying, etc. The importance of XPS has grown tremendously in recent years due to the rise of modern near-ambient XPS (NAP-XPS) techniques that are able to measure the catalyst directly in realistic gaseous environments [103], yet the application of XPS in liquid environment is far more challenging. Nonetheless, few specially designed electrochemical cells allowed successfully apply XPS in liquid environment and perform *in situ*/*in operando* measurements [104–106].

Spectroscopic techniques provide invaluable chemical information, but they are relatively slow and possess a lower signal-to-noise ratio in comparison to diffraction measurements. As an alternative, high-energy X-ray diffraction (XRD) was shown to be an ideal probe to quantitatively study the crystal structure of Pt-based fuel cell catalysts in real time in electrochemical environment [102,107].

Compared with the above techniques, infra-red (IR) spectro-electrochemistry also allows *in situ/in operando* studies on electrified interfaces but is rather focused on the detection of different adsorption sites on the catalyst surface during ORR thus providing additional information on the course of the reaction [108,109]. The advantages of *in situ/in operando* IR spectro-electrochemistry is its high sensitivity and fast analysis.

Understanding corrosion of catalyst is of further pivotal importance. Both Pt and alloying metals tend to dissolve in the PEMFC operating range. However, the onset of dealloying is different for different elements [25]. The success in understanding of catalyst electrochemical dissolution in simulated fuel cell environment in recent years can be attributed to successfully coupling the so-called scanning flow cell (SFC) to an inductively coupled plasma mass spectrometer (ICP-MS) [110,111]. This setup based on online mass spectrometry allows monitoring extremely low concentrations of dissolved metal in the electrolyte during electrochemical treatment while simultaneously monitoring the current response. Effect of temperature, scan rate, pH, potential can be carefully investigated [29,111,112].

In situ/in operando studies have been proven to provide insightful information into the catalyst morphology, composition and chemical state of individual elements under reaction conditions bringing the current frontiers of knowledge to the next level. However, despite the impressive progress, there are still many factors hindering the full understanding of catalyst

behavior in fuel cells. One of them is that the multiple factors govern the catalytic activity and stability and no single method is capable to provide a complete picture of the catalyst behaviour. Thus, the simultaneous combination of several *in situ/in operando* instruments is expected to obtain a more coherent picture of relationship between the structure, activity and stability of electrocatalysts. The second problem is the significant gap between a real PEMFC device and an idealized electrochemical cell designed specifically for a particular technique. Many challenges and opportunities thus persist, and the contributions of *in situ*/*in operando* characterization to decipher the working mechanisms and degradation pathways of electrocatalysts in real PEMFCs are yet to be overcome.

3. Results

Apart from overcoming the ORR catalyst cost-efficiency and durability issues it is important in parallel to develop a simple and fast method for its scalable and economically viable production which is, at the same time, able to provide fine control over critical parameters such as morphology, structure, composition profile, etc. The majority of state-of-the-art cathode catalysts discussed above were prepared using a standard wet-chemical synthesis. This method, however, has certain drawbacks, such as a limited range of achievable materials and high price. Moreover, catalysts produced by wet-chemical synthesis often contain surfactants which are not easy to get rid of.

In the presented thesis that is composed of 13 the most important papers (denoted as P1-P13) we are focused on PEMFC cathode catalysts prepared by magnetron sputtering. Magnetron sputtering is one of the physical vapor deposition techniques for the preparation of thin films. It is a standard industrial technique that can be a suitable candidate for this call. Plenty of material combinations at different compositions are accessible for the sputtering technology. Moreover, the variation of deposition parameters allows precise, cheap and environmentally friendly preparation of an exceptionally broad range of surfactant-free alloy catalysts. Indeed, the magnetron sputtering technique is attracting a renewed interest in the field of PEMFCs [113–117].

The results presented here are divided into two chapters classified topically as follow:

- Activity of Pt-based bimetallic alloys
- Stability of platinum and Pt-based bimetallic alloys

3.1. Activity of Pt-based bimetallic alloys

Recently in the Department of Surface and Plasma Physics at Faculty of Mathematics and Physics of Charles University we developed a very efficient Pt-CeO_2 material for the PEMFC anode [118]. Such material is based on nanoporous Pt-CeO_2 thin films prepared by simultaneous magnetron sputtering of Pt and CeO_2 allowing the production of oxide layers continuously doped with Pt atoms during the growth. Spectroscopic characterization revealed that, in the Pt-CeO_2 catalyst Pt is mostly present as single platinum atoms [118]. Combining Density Functional Theory (DFT) studies with model experiments in UHV we determined that such Pt species on the surface are Pt^{2+} cations that reside in a square-planar $[O^{2-}]_4$ coordination site located at {100} nanofacets of CeO_2 [119]. The unprecedentedly low Pt loading on cheap

cerium oxide support showing significant catalytic activity for HOR makes this material of eminent economical interest.

In order to show the great potential of the promising technology of magnetron sputtered catalyst for fuel cell application, we decided to use it also for the preparation of cathode catalysts. The work **P-1** presents our first study of the PEMFC made exclusively from thin film catalysts. We tested a single cell catalysed by combining the Pt-CeO_2 anode and a new PtCo alloy cathode. The $Pt_{50}Co_{50}$ alloy layer was prepared by simultaneous magnetron sputtering from two individual targets: Pt and Co. FC tests revealed high power density of 125 mW cm^{-2} with loading of 50 μg_{Pt} cm^{-2} for whole MEA (2 and 48 μg_{Pt} cm^{-2} for the anode and the athode, respectively) giving Pt mass activity of 2.5 kW g^{-1}. The results demonstrated that magnetron sputtering can be successfully applied for the efficient cathode catalyst preparation.

To gain insights into the activity of magnetron co-sputtered Pt-Co layer we performed its complete characterization using powerful surface sensitive techniques. The comprehensive investigation of the magnetron prepared PtCo catalyst thin film catalyst by both experimental and theoretical methods is presented in **P-2**. The microscopy characterization revealed the nanostructured character of the Pt-Co layer consisting of homogeneously distributed polycrystalline grains with the average size around 8 nm. SRPES and XPS data have demonstrated that Co affects the electronic properties of the Pt-rich surface resulting in the d-band center shift as well as shifts of the Pt 4f, Co 3p and Co 2p photoelectron peak energies. This is consistent with the general theory of ORR activity enhancement in case of bimetallic alloys.

To achieve a deeper understanding of the structure of thin films catalyst, we further carried out theoretical calculations for model PtCo NPs. Optimization of the chemical ordering by density functional theory (DFT) calculations showed that the gain in the energy corresponding to the segregation of Pt on the surface (preferentially on corner and edge positions) is the driving force in the stabilization of PtCo nanoparticles. According to experiment, the density of valence states of surface atoms in PtCo nanostructures is shifted by 0.3 eV to higher energies, which supported spectroscopic measurements.

Next, Pt-Ni and Pt-Y alloys prepared by magnetron sputtering were studied as they pose the cathode catalytic material of the highest interest nowadays as highlighted in the section 2.2.3. In **P-3** we investigated co-sputtered Pt-Ni alloy. The FC tests revealed higher mass activity of the $Pt_{50}Ni_{50}$ alloy cathode than that of pure sputtered platinum. We further investigated the correlation between Pt-Ni composition and its catalytic properties. Fine power adjustment on magnetrons allowed to deposit Pt_xNi_{100-x} ($0 \leq x \leq 100$) alloys with precise composition and at

the same time with identical thickness of 10 nm and similar morphologies in order to avoid morphology influence on the ORR activity. The influence of the composition on the morphology and structure of the catalytic films was further evaluated using a combination of powerful characterization techniques. The thickness of all catalysts were estimated to be around 10 nm and the roughness was ~0.35 nm and ~6 nm in vertical and spatial dimensions, respectively. XRD confirmed the alloy nature of all deposited films with one crystalline phase of the face-centered cubic (fcc) PtNi. The linear dependence in the construction of Pt lattice was observed with increasing the amount of Ni in the alloy in accordance to the Vegard's law.

The selected Pt_xNi_{100-x} catalysts (x = 25, 50, 75 and 100) were further tested in an electrochemical cell and as a cathode in a single-cell. Cyclic voltammetry was applied to determine an ECSA of the selected alloys. ECSA gradually increases with increasing Ni concentration in the alloy. The higher ECSA for Pt_xNi_{100-x} alloys in comparison to pure Pt was explained by the formation of the so-called Pt-skeleton with higher concentration of low coordinated Pt atoms due to nickel leaching from the surface. The alloys showed a significant increase in the specific power (power per Pt loading) comparing to the pure Pt thin films and a commercial Pt nanoparticle catalyst in a single cell. Particularly, the $Pt_{25}Ni_{75}$ sample exhibited the highest specific power of 24 kW/g_{Pt} which is almost 2-fold higher than that for pure Pt films (14 kW/g_{Pt}) and almost 10-fold higher with respect to the benchmark commercial Pt catalyst (2.3 kW/g_{Pt}). The activity enhancement was explained by the interplay of the intrinsic activity due to alloy formation (Pt lattice shrinking) and the expansion of the electroactive surface area as a result of surface dealloying.

The works **P-4** and **P-5** deal with systematic investigation of Pt_3Y cathode catalyst. In contrast to previous studies, the Pt_3Y film was produced by magnetron sputtering from the alloy target. In **P-4** we reported the activity increase about seven times comparing to that of polycrystalline Pt using RDE measurements in the half-cell in acidic electrolyte at 0.90 V_{RHE}. In turn, in **P-5** the Pt_3Y cathode catalyst was tested as a cathode in a real fuel cell device and show two-time enhancement over pure platinum. The catalysts performance in a real fuel cell is known to be significantly affected by the mass and charge transport limitations and harsh working environment, resulting in lower activity than in case of well-defined half-cell conditions [120].

A detailed photoemission analysis of the sputtered Pt_3Y catalyst surface, using surface sensitive SRPES was provided to examine the nature of the alloy surface. The Pt_3Y catalyst surface was investigated before and after acid treatment. The increased activity of Pt_3Y films was explained by the formation of a three monolayer thick Pt overlayer due to the removal

most of the yttrium oxide from the surface. The DFT calculations showed the core level shifts (CLS) for a surface atom in Pt(111) and Pt atom in a $Pt_3Y(111)$ are -0.35 eV and -0.20 eV, respectively.

Overall results described in this chapter demonstrate the utility of the co-sputtering process to produce active alloys catalyst of specific composition in a controllable way for the PEMFC cathode. Taking into account our previous results on the Pt-CeO_2 anode catalyst, MEA made from thin film catalysts on both PEMFC electrodes prepared by a single method simplifies and accelerates the scalable manufacturing process. Moreover, simplicity, scalability and economic viability of magnetron sputter deposition together with complete omission of undesirable surfactants underlines undisputable advantage of this approach.

3.2. Stability of platinum and Pt-based bimetallic alloys

In parallel advanced *in-situ/in operando* experimental methods were used to directly explore the physics and chemistry behind the activity and stability of fuel cell cathode catalysts prepared by magnetron sputtering. When deposited onto a flat surface, the relative flat character of the thin film catalyst permits the use of electrochemical AFM for *in situ* characterization of the catalyst morphology during simulated electrochemical aging. A combination of powerful *ex situ* spectroscopic analyses such as EDX, XPS and SRPES with *in situ* EC-AFM technique was effectively employed to provide step-by-step insight into the degradation mechanisms of the PtCo (**P-6**), PtNi(**P-7**) and PtCu(**P-8**) thin film catalysts. A cyclic voltammetry was applied to simulate catalyst aging inside the electrochemical cell integrated into AFM. EC-AFM thus allowed investigating electrochemical reactions on the surface of the catalyst by capturing CV curves and simultaneously visualizing changes in its morphology. Before and after electrochemical tests catalyst was thoroughly investigated with *ex situ* spectroscopic techniques to reveal possible changes in catalyst chemical composition induced by electrochemical cycling.

The results showed that the bimetallic catalysts deteriorate tremendously, when operated at harsh conditions (cycling to upper potential 1.3 and 1.5 V_{RHE}) that a fuel cell may experience during an automotive startup/shutdown mode. Such relatively high oxidation potentials during electrochemical cycling were found to gradually and irreversibly destroy the alloy catalyst due to strong Co (**P-6**), Ni (**P-7**), Cu (**P-8**) leaching Moreover, a significant catalyst coarsening was observed which was interconnected with a decrease of the catalyst active surface area calculated from corresponding CVs.

More thorough investigation of bimetallic catalyst degradation during electrochemical cycling was conducted for PtCu (**P-8**) and PtNi (**P-9**) alloys where we investigated the potential-dependent behavior of the bimetallic catalysts during electrochemical cycling to different upper potential limits simulating different operational regimes of PEMFC. In addition to EC-AFM, complementary *in situ* infrared reflection absorption spectroscopy (EC-IRRAS) with CO as probe molecule was used. It enabled to explore the nature of different adsorption sites at the surface of the catalyst and allowed us to follow *in situ* reactions on the bimetallic surface during its degradation.

For the Pt-Cu catalyst in **P-8** three upper potentials were used: 0.8, 1.0 and 1.4 V_{RHE}. In turn for PtNi in **P-9** we systematically investigated the stability, structural transformations and adsorption properties of PtNi nanoalloy thin film electrocatalysts during stepwise increase of upper potential from 0.9 to 1.5 V_{RHE}. Thorough potential control enabled to reveal an onset potential for significant bimetallic catalyst degradation. EC-AFM results showed that, regardless of the upper potential limit, the formation of cracks was observed already at the beginning of electrochemical cycling, which was attributed to the leaching of non-noble metal (Cu, Ni) from the alloy. With the increase of cycling number, only minor structural changes occur up to an upper potential limit of 1.1 $V_{RHE.}$ At these conditions *in situ* IR results reveal that in addition to regular on-top CO adsorbed on Pt sites, CO adsorbed at low-coordinated Pt atoms, that are released upon leaching of non-noble metal from the surface layer of the bimetallic alloy particles, were detected. In turn, drastic changes in the morphology and surface composition of the bimetallic nanoalloy particles occurred upon potential cycling to 1.2 V_{RHE} and higher. The CO spectra in EC-IRRAS were nearly identical to those obtained on rough Pt surfaces indicating absence of alloying metal even in subsurface layers of the alloy due to strong dealloying. In addition, EC-AFM showed significant coarsening of these catalytic layers.

The main reason for substantial catalyst degradation at potentials 1.2 V_{RHE} and higher was find to be strong oxidation of platinum and its subsequent reduction at each cycle. The onset of Pt oxidation occurs at around 0.8 V_{RHE}, however, after around 1.2 V_{RHE} a so-called place-exchange between Pt and O atoms occurs which leads to the formation of bulk Pt-oxides. The formation and reduction of these oxides at each cycle lead to catalyst surface restructuring which uncovers less noble metal (previously buried under a protective platinum overlayer) and stimulate its further dissolution. Moreover, Pt dissolution/redeposition is enhanced at these cycling condition which in turn stimulates Ostwald ripening-based catalyst coarsening.

Our efforts were further devoted to distinguishing between different mechanisms which occur during electrochemical degradation of bimetallic alloy catalyst namely dealloying, Ostwald ripening and coalescence.

At first, the EC-AFM was applied to characterize *in situ* the potential dependent roughening of the pure platinum thin film catalyst during electrochemical cycling. For the first time, we apply the quantitative analysis based on AFM results to describe the surface coarsening kinetics during the electrochemical degradation of platinum (**P-10**). The comprehensive quantitative analysis was obtained by computing common roughness descriptors such as the root mean square roughness, the correlation length, and the critical exponents. The results showed that when the $E_U = 1.0\ V_{RHE}$, the Pt film surface did not change significantly. The growth and the coarsening exponents were close to zero, meaning that the interface stays statistically self-similar during the entire cycling procedure. The ECSA calculated from the CV curves was invariable as well, confirming relative electrochemical stability of platinum at aforementioned conditions at early stages of degradation (total 2000 cycles we apply in this study). When E_U increased to 1.3 and 1.5 $V_{RHE,}$ the Pt morphology evolved significantly with the number of cycles. The morphology correlations in the lateral dimension propagated with the same coarsening exponent $1/z = 0.16 \pm 0.02$ for both 1.3 V_{RHE} and 1.5 V_{RHE}. In turn, the growth exponent β, which corresponds to correlations in the vertical dimension, was 0.22 ± 0.04 for 1.3 V_{RHE} and 0.40 ± 0.02 for 1.5 V_{RHE}, indicating that the film evolves faster in the vertical direction than in the lateral one when the upper potential is 1.5 V_{RHE}. The ECSA decreased by about 10% and 20% during the entire cycling procedure for $E_U = 1.3$ and $E_U = 1.5\ V_{RHE}$, respectively, indicating a good correlation with the development of roughness. The coarsening of platinum at higher potentials was explained by a combined influence of Ostwald ripening and coalescence. However, we could not distinguish individual contributions from these processes because they occur simultaneously, resulting in scaling exponents different from those theoretically predicted using idealized conditions.

In order to obtain better statistics together with higher resolution, a special electrochemical cell for *in situ* grazing incidence small-angle X-ray scattering (GISAXS) was developed, which allowed to combine electrochemical studies and GISAXS in half-cell geometry. *In situ* electrochemical GISAXS permitted to investigate the in-depth mean morphological variation of the catalyst by probing a large sample area (around 4 mm^2) in a relatively short time, providing very good statistical accuracy and very high resolution and thus complement EC-AFM results. The work **P-11** describes the electrochemical cell design and contains the study of the morphological evolution of a pure platinum catalyst layer using identical experimental

conditions to those in **P-10**. The horizontal and vertical cuts of experimentally obtained scattering patterns were analysed, providing information about the in-plane and out-plain morphological evolution of Pt during electrochemical aging. At E_U equal to 1.0 V_{RHE}, the expected stability of the catalyst was confirmed during 2000 CV cycles. On the other hand, at E_U equal to 1.5 V_{RHE}, the morphological modification affecting the system was deciphered: in the first stage, the coalescence of Pt particles has been highlighted from a preferential growth in Pt NPs size occurring along the plane of the surface, together with a consequent, slight, thinning of the Pt film. In a later stage, it was possible to detect the particle growth induced by Ostwald ripening mechanism. The statistical parameters evolution such as mean particle size, roughness, and correlation length calculated from *in situ* GISAXS measurements showed trends identical to those obtained in **P-10** using *in situ* EC-AFM during electrochemical cycling, proving the reliability of the developed setup. The work described in **P-11**, however, provides a more advanced picture about platinum catalyst coarsening. The applicability of this setup can also be easily extended to other research fields such as battery or super capacitors where electrochemical process is of significant importance, and the investigations of the electrode interface layers during operation are essential.

Finally, the combination of both *in situ* EC-AFM and *in situ* GISAXS was apply in **P-12** to investigate the potential-dependent degradation of the PtNi bimetallic catalyst. In addition to PtNi coarsening, attention was paid to its dealloying. For that, electrochemical scanning flow cell with online detection by ICP-MS was additionally applied to provide insights into the dissolution of both Pt and Ni during electrochemical cycling. The study revealed a clear correlation between the upper potential limit, PtNi catalyst dealloying and its morphological behaviour. The results show that at the low upper potential conditions (0.6 and 1.0 V_{RHE}), the PtNi catalyst is affected only by negligible Ni dissolution at early stages of cycling and more or less preserves its morphology during the entire cycling procedure, which is in line with previous studies. On the contrary, dramatic changes in the morphology of the PtNi layers occur at higher cycling potentials (1.3 and 1.5 V_{RHE}). At these upper potentials Ni dissolution occurred rapidly and Pt dissolution was progressively induced: the strong dealloying at the early stages of cycling was exchanged with strong coarsening of catalyst particles at later stages. By means of powerful *in situ* analysis, it was possible to establish that this exchange occurs after ~300 cycles for cycling to 1.3 $V_{RHE,}$ while in the harsher conditions (cycling to 1.5 V_{RHE}), it starts already after few tenths of cycles. Moreover, with detailed GISAXS analysis, further supported by AFM measurements, it was possible to assign particle coarsening at the later stage of cycling to the Ostwald ripening process. The combination of three *in situ*

techniques described above provided a full time-resolved picture of PtNi bimetallic catalyst deterioration during electrochemical ageing and currently applied to investigate the composition-dependent degradation of the Pt-Ni ORR catalyst.

During electrochemical cycling repeating oxidation and reduction of the catalyst surface occur. In order to get spectroscopic insights on what is going on bimetallic surface during electrochemical cycling we simulated oxidation and reduction of the PtNi catalyst by simply exposing it to changeable 5 mbar of oxygen and 5 mbar of hydrogen atmosphere. In **P-13** we investigated the temperature-dependent surface restructuring of the PtNi thin film catalyst in response to five cycles of alternating oxidation and reduction atmospheres. The surface restructuring in response to reactive media were monitored by surface sensitive SRPES technique and more bulk sensitive XPS technique without sample exposure to air. The experimental results were substantiated by theoretical calculations of model PtNi nanoalloys.

The results revealed that under oxidation environment the PtNi alloy oxidized on the surface through the formation of Ni (Ni^{ox}) and Pt (Pt^{ox}) oxides. Upon increasing the temperature, the oxides contribution on the surface increased with complete disappearance of the metallic nickel (Ni^{met}) signal at 523 K. Beyond that, the foregoing oxidation forced Ni atoms to segregate to the surface due to the stronger bonding of O to Ni as compared to Pt, as substantiated by suppression of the Pt 4f signal. Under subsequent reducing atmosphere Pt^{ox} and Ni^{ox}, are reduced back to metallic states (Pt^{met}, Ni^{met}). Consequently, the reduction also causes back diffusion of Ni atoms into the alloy. The series of five oxidation/reduction cycles led to an oscillatory behaviour of the surface composition. The changes were qualitatively reversible; quantitatively, however, the average composition was contentiously shifting towards nickel enrichment at elevated cycling temperatures. The enrichment of Ni species on the surface after an interaction with the reactive environments suppresses PtNi alloy on the surface which is critical for its high electrocatalytic performance. Moreover, we observed significant catalyst coarsening after five oxidation/reduction cycles at 523 K assigned to enhanced atomic (Ostwald ripening) and grains (coalescence) mobility at elevated temperatures in gaseous atmospheres. The results provided valuable insights into the PtNi alloy surface chemistry under switched reactive environments.

The results described in this section allowed deciphering the time-resolved evplution of bimetallic alloys during electrochemical aging simulated in a half-cell thus contributing to the advance understanding of cathode catalyst behavior under PEMFC operating conditions.

4. Summary

As environmental and economic concerns continue to grow, reducing reliance on fossil fuels through harvesting low or even zero-emission energy becomes increasingly important for our society. This is substantiated by the recent political will to authorize approaching towards achieving zero carbon emissions by 2050. Hydrogen-fueled PEMFCs are the most promising and flexible option for the above outlined call due to their environmental sustainability, high energy density, high energy-conversion efficiency and low operating temperatures. Although endowing with great potential and already showing partial success in the market, PEMFCs are facing some technological hurdles which require extensive research and development to be overcome. Among them cost-efficiency and stability of cathode catalysts in fuel cells pose the greatest challenge. Extensive academic and industrial research efforts are already made for conceiving new efficient catalysts with major focus on alloying of Pt with cheaper elements. A variety of Pt-based bimetallic catalyst have been developed and tested. Some of them have already entered the market, while some are still under investigation.

The long-term stability of Pt-based catalyst as a second drawback for PEMFCs commercialization has become the most important challenge to be addressed. The degradation mechanisms are well recognized for state-of-the-art Pt/C systems. However, novel materials may suffer from unpredictable new and even more complicated degradation mechanisms. With the development of powerful *in situ*/*in operando* techniques in recent years, PEMFC catalyst degradation has received an increased interest. *In situ/in operando* studies are expected to provide valuable insights into the catalyst degradation mechanisms under reaction conditions bringing the current frontiers of knowledge into the next level.

It can be expected that continued intensive fundamental research and commercial development will eventually lead to the reduced cost and extended lifetime of cathode catalyst in PEMFCs. It is thus vital in parallel to develop the method for scalable and economically viable catalyst production.

In this regard the presented thesis demonstrates the utility of the magnetron co-sputtering process to produce active alloy catalysts of specific composition in a controllable way for the PEMFCs cathode. Pt-Ni, PtCo and Pt_3Y alloys prepared by magnetron sputtering were tested as cathode catalysts in the real PEMFC devise and showed enhanced activity in comparison to pure platinum. Moreover, using advanced *in-situ/in operando* experimental methods we obtained important insights in terms of the correlation between the structure, activity and stability of bimetallic catalysts. A combination of *in-situ/in operando* state-of-art techniques as

EC-AFM, GISAXS, ICP-MS, NAP-XPS and infrared EC-IRRAS were applied to decipher the time-resolved behavior of bimetallic alloys during electrochemical aging simulated in the half-cell. Interplay between dealloying, particle coalescence and Ostwald ripening was described in details contributing to the advance understanding of magnetron sputtered cathode catalyst behavior under PEMFC operating conditions.

The presented results demonstrate a complicated degradation mechanisms of cathode catalysts depending on operation conditions of a PEMFC. A further rigorous research is still required in order to increase understanding of these mechanisms and propose effective mitigation strategies. This is essential for the development of the cathode catalyst that satisfy all criteria for PEMFC commercialization. Overall, the global investment, political will and extensive research and development all together suggest that the hydrogen fuel cell market is expected to show a phenomenal growth in the future accompanied with incremental market entry.

5. References

[1] Europian Commission, 2050 long-term strategy, (2019). https://ec.europa.eu/clima/policies/strategies/2050_en.

[2] W. Vielstich, A. Lamm, H.A. Gasteiger, Eds., Handbook of fuel cells: Fundamentals, technology, applications, Wiley, 2003.

[3] C.K. Dyer, Fuel cells for portable applications, J. Power Sources. 106 (2002) 31–34. doi:10.1016/S0378-7753(01)01069-2.

[4] B.G. Pollet, S.S. Kocha, I. Staffell, Current status of automotive fuel cells for sustainable transport, Curr. Opin. Electrochem. 16 (2019) 90–95. doi:10.1016/j.coelec.2019.04.021.

[5] P. Lin, P. Zhou, C.W. Wu, A high efficient assembly technique for large PEMFC stacks: Part I. Theory, J. Power Sources. 194 (2009) 381–390. doi:10.1016/j.jpowsour.2009.04.068.

[6] A.G. Olabi, T. Wilberforce, M.A. Abdelkareem, Fuel cell application in the automotive industry and future perspective, Energy. 214 (2021) 118955. doi:10.1016/j.energy.2020.118955.

[7] Y. Wang, B. Seo, B. Wang, N. Zamel, K. Jiao, X.C. Adroher, Fundamentals, materials, and machine learning of polymer electrolyte membrane fuel cell technology, Energy AI. 1 (2020) 100014. doi:https://doi.org/10.1016/j.egyai.2020.100014.

[8] Y. Wang, D.F. Ruiz Diaz, K.S. Chen, Z. Wang, X.C. Adroher, Materials, technological status, and fundamentals of PEM fuel cells – A review, Mater. Today. 32 (2020) 178–203. doi:10.1016/j.mattod.2019.06.005.

[9] S. Hardman, G. Tal, Who are the early adopters of fuel cell vehicles?, Int. J. Hydrogen Energy. 43 (2018) 17857–17866. doi:10.1016/j.ijhydene.2018.08.006.

[10] Hyundai Nexo fuel cell vehicle, (2020). https://www.hyundaiusa.com/us/en/vehicles/nexo.

[11] Toyota Mirai fuel cell electric vehicle, (2020). https://www.toyota.com/mirai/fcv.html.

[12] Honda Clarity fuel cell – hydrogen-powered car, (2020). https://automobiles.honda.com/clarity-fuel-cell.

[13] Alstom's hydrogen train enters regular passenger service in Austria, (2020). https://www.alstom.com/press-releases-news/2020/9/alstoms-hydrogen-train-enters-regular-passenger-service-austria.

[14] Successful year and a half of trial operation of the world's first two hydrogen trains, next project phase begins, (2020). https://www.alstom.com/press-releases-news/2020/5/successful-year-and-half-trial-operation-worlds-first-two-hydrogen.

[15] The Telegraph. Hydrogen fuel cell trains to run on British railways from 2022, (2019). https://www.telegraph.co.uk/cars/news/hydrogen-fuel-cell-trains-run-british-railways-2022/.

[16] A. Baroutaji, T. Wilberforce, M. Ramadan, A.G. Olabi, Comprehensive investigation on hydrogen and fuel cell technology in the aviation and aerospace sectors, Renew. Sustain. Energy Rev. 106 (2019) 31–40. doi:10.1016/j.rser.2019.02.022.

[17] Cross-industry collaboration is set to unlock the technology's potential for aviation, (2020). https://www.airbus.com/newsroom/news/en/2020/10/hydrogen-fuel-cell-cross-industry-collaboration-potential-for-aviation.html.

[18] U.S. Department of Energy, DOE hydrogen and fuel cells program record. Automotive fuel cell targets and status, (2020). https://www.hydrogen.energy.gov/program_records.html.

[19] U.S. Department of Energy, DOE technical targets for polymer electrolyte membrane fuel cell components, (2015). https://www.energy.gov/eere/fuelcells/doe-technical-targets-polymer-electrolyte-membrane-fuel-cell-components.

[20] W. Vielstich, H.A. Gasteiger, H. Yokokawa Eds., Handbook of fuel cells: Advances in electrocatalysis, material, diagnostics and durability, Wiley, 2009.

[21] J.K. Nørskov, J. Rossmeisl, A. Logadottir, L. Lindqvist, J.R. Kitchin, T. Bligaard, H. Jónsson, Origin of the overpotential for oxygen reduction at a fuel-cell cathode, J. Phys. Chem. B. 108 (2004) 17886–17892. doi:10.1021/jp047349j.

[22] C.A. Reiser, L. Bregoli, T.W. Patterson, J.S. Yi, J.D. Yang, M.L. Perry, T.D. Jarvi, A reverse-current decay mechanism for fuel cells, Electrochem. Solid-State Lett. 8 (2005) A273–A276. doi:10.1149/1.1896466.

[23] U.S. Department of Energy. Accelerated stress test and polarization curve protocols for PEM fuel cells, (2013). https://www.energy.gov/eere/fuelcells/downloads/fuel-cell-tech-team-accelerated-stress-test-and-polarization-curve.

[24] J.C. Meier, C. Galeano, I. Katsounaros, J. Witte, H.J. Bongard, A.A. Topalov, C. Baldizzone, S. Mezzavilla, F. Schüth, K.J.J. Mayrhofer, Design criteria for stable Pt/C fuel cell catalysts, Beilstein J. Nanotechnol. 5 (2014) 44–67. doi:10.3762/bjnano.5.5.

[25] M. Pourbaix, Atlas of electrochemical equilibria in aqueous solutions, (2nd English Ed.), Natl. Assoc. Corros. Eng. (1974) 551 pages.

[26] F. Chang, G. Yu, S. Shan, Z. Skeete, J. Wu, J. Luo, Y. Ren, V. Petkov, C.J. Zhong, Platinum-nickel nanowire catalysts with composition-tunable alloying and faceting for the oxygen reduction reaction, J. Mater. Chem. A. 5 (2017) 12557–12568. doi:10.1039/c7ta03266h.

[27] K. Yasuda, A. Taniguchi, T. Akita, T. Ioroi, Z. Siroma, Platinum dissolution and deposition in the polymer electrolyte membrane of a PEM fuel cell as studied by potential cycling, Phys. Chem. Chem. Phys. 8 (2006) 746–752. doi:10.1039/B514342J.

[28] A.A. Topalov, S. Cherevko, A.R. Zeradjanin, J.C. Meier, I. Katsounaros, K.J.J. Mayrhofer, Towards a comprehensive understanding of platinum dissolution in acidic media, Chem. Sci. 5 (2014) 631–638. doi:10.1039/C3SC52411F.

[29] S. Cherevko, G.P. Keeley, S. Geiger, A.R. Zeradjanin, N. Hodnik, N. Kulyk, K.J.J. Mayrhofer, Dissolution of platinum in the operational range of fuel cells, ChemElectroChem. 2 (2015) 1471–1478. doi:10.1002/celc.201500098.

[30] S.R. Challa, A.T. Delariva, T.W. Hansen, S. Helveg, J. Sehested, P.L. Hansen, F. Garzon, A.K. Datye, Relating rates of catalyst sintering to the disappearance of individual nanoparticles during Ostwald ripening, J. Am. Chem. Soc. 133 (2011) 20672–20675. doi:10.1021/ja208324n.

[31] K.H. Lim, H.-S. Oh, S.-E. Jang, Y.-J. Ko, H.-J. Kim, H. Kim, Effect of operating conditions on carbon corrosion in polymer electrolyte membrane fuel cells, J. Power Sources. 193 (2009) 575–579. doi:10.1016/j.jpowsour.2009.04.006.

[32] L. Castanheira, W.O. Silva, F.H.B. Lima, A. Crisci, L. Dubau, F. Maillard, Carbon corrosion in proton-exchange membrane fuel cells: Effect of the carbon structure, the degradation protocol, and the gas atmosphere, ACS Catal. 5 (2015) 2184–2194. doi:10.1021/cs501973j.

[33] J.C. Meier, C. Galeano, I. Katsounaros, A.A. Topalov, A. Kostka, F. Schüth, K.J.J. Mayrhofer, Degradation mechanisms of Pt/C fuel cell catalysts under simulated start-stop conditions, ACS Catal. 2 (2012) 832–843. doi:10.1021/cs300024h.

[34] M. Escudero-Escribano, K.D. Jensen, A.W. Jensen, Recent advances in bimetallic electrocatalysts for oxygen reduction: design principles, structure-function relations and active phase elucidation, Curr. Opin. Electrochem. 8 (2018) 135–146. doi:10.1016/j.coelec.2018.04.013.

[35] D. Banham, T. Kishimoto, Y. Zhou, T. Sato, K. Bai, J. Ozaki, Y. Imashiro, S. Ye, Critical advancements in achieving high power and stable nonprecious metal catalyst–based MEAs for real-world proton exchange membrane fuel cell applications, Sci. Adv. 4 (2018) eaar7180. doi:10.1126/sciadv.aar7180.

[36] E. Proietti, F. Jaouen, M. Lefèvre, N. Larouche, J. Tian, J. Herranz, J.-P. Dodelet, Iron-based cathode catalyst with enhanced power density in polymer electrolyte membrane fuel cells, Nat. Commun. 2 (2011) 416. doi:10.1038/ncomms1427.

[37] L. Osmieri, J. Park, D.A. Cullen, P. Zelenay, D.J. Myers, K.C. Neyerlin, Status and challenges for the application of platinum group metal-free catalysts in proton-exchange membrane fuel cells, Curr. Opin. Electrochem. 25 (2021) 100627. doi:10.1016/j.coelec.2020.08.009.

[38] V. Goellner, C. Baldizzone, A. Schuppert, M.T. Sougrati, K. Mayrhofer, F. Jaouen, Degradation of Fe/N/C catalysts upon high polarization in acid medium, Phys. Chem. Chem. Phys. 16 (2014) 18454–18462. doi:10.1039/C4CP02882A.

[39] T. Yu, D.Y. Kim, H. Zhang, Y. Xia, Platinum concave nanocubes with high-index facets and their enhanced activity for oxygen reduction reaction, (2011) 2825–2829. doi:10.1002/ange.201007859.

[40] B.Y. Xia, H. Bin Wu, X. Wang, X. Wen, D. Lou, Highly concave platinum nanoframes with high-index facets and enhanced electrocatalytic properties, (2013) 12563–12566. doi:10.1002/ange.201307518.

[41] C.M. Sánchez-Sánchez, J. Solla-Gullón, F.J. Vidal-Iglesias, A. Aldaz, V. Montiel, E. Herrero, Imaging structure sensitive catalysis on different shape-controlled platinum nanoparticles, J. Am. Chem. Soc. 132 (2010) 5622–5624. doi:10.1021/ja100922h.

[42] J. Chen, B. Lim, E.P. Lee, Y. Xia, Shape-controlled synthesis of platinum nanocrystals for catalytic and electrocatalytic applications, Nano Today. 4 (2009) 81–95. doi:10.1016/j.nantod.2008.09.002.

[43] Z.-Y. Zhou, N. Tian, Z.-Z. Huang, D.-J. Chen, S.-G. Sun, Nanoparticle catalysts with high energy surfaces and enhanced activity synthesized by electrochemical method, Faraday Discuss. 140 (2009) 81–92. doi:10.1039/B803716G.

[44] Q. Shao, K. Lu, X. Huang, Platinum group nanowires for efficient electrocatalysis, Small Methods. 3 (2019) 1800545. doi:10.1002/smtd.201800545.

[45] Y. Chen, T. Cheng, W.A. Goddard III, Atomistic explanation of the dramatically improved oxygen reduction reaction of jagged platinum nanowires, 50 times better than Pt, J. Am. Chem. Soc. 142 (2020) 8625–8632. doi:10.1021/jacs.9b13218.

[46] R. Wang, D.C. Higgins, A. Hoque, D. Lee, F. Hassan, Z. Chen, Controlled growth of platinum nanowire arrays on sulfur doped graphene as high performance electrocatalyst, Sci. Rep. (2013) 1–7. doi:10.1038/srep02431.

[47] M. Li, Z. Zhao, T. Cheng, A. Fortunelli, C.-Y. Chen, R. Yu, Q. Zhang, L. Gu, B. V Merinov, Z. Lin, E. Zhu, T. Yu, Q. Jia, J. Guo, L. Zhang, W.A. Goddard, Y. Huang, X. Duan, Ultrafine jagged platinum nanowires enable ultrahigh mass activity for the oxygen reduction reaction, Science. 354 (2016) 1414 LP-1419. doi:10.1126/science.aaf9050.

[48] C. Koenigsmann, W. Zhou, R.R. Adzic, E. Sutter, S.S. Wong, Size-dependent enhancement of electrocatalytic performance in relatively defect-free, processed ultrathin platinum nanowires, Nano Lett. 10 (2010) 2806–2811. doi:10.1021/nl100718k.

[49] W.J. Khudhayer, N.N. Kariuki, X. Wang, D.J. Myers, A.U. Shaikh, T. Karabacak, Oxygen reduction reaction electrocatalytic activity of glancing angle deposited platinum nanorod arrays, J. Electrochem. Soc. 158 (2011) B1029. doi:10.1149/1.3599901.

[50] W. Shimizu, K. Okada, Y. Fujita, S. Zhao, Y. Murakami, Platinum nanowire network with silica nanoparticle spacers for use as an oxygen reduction catalyst, J. Power Sources. 205 (2012) 24–31. doi:10.1016/j.jpowsour.2011.12.053.

[51] V.T.T. Ho, N.G. Nguyen, C.-J. Pan, J.-H. Cheng, J. Rick, W.-N. Su, J.-F. Lee, H.-S. Sheu, B.-J. Hwang, Advanced nanoelectrocatalyst for methanol oxidation and oxygen reduction reaction, fabricated as one-dimensional pt nanowires on nanostructured robust $Ti_{0.7}Ru_{0.3}O_2$ support, Nano Energy. 1 (2012) 687–695. doi:10.1016/j.nanoen.2012.07.007.

[52] S.M. Alia, G. Zhang, D. Kisailus, D. Li, S. Gu, K. Jensen, Y. Yan, Porous platinum nanotubes for oxygen reduction and methanol oxidation reactions, Adv. Funct. Mater. 20 (2010) 3742–3746. doi:10.1002/adfm.201001035.

[53] S. Ci, J. Zou, G. Zeng, S. Luo, Z. Wen, Single crystalline Pt nanotubes with superior electrocatalytic stability, J. Mater. Chem. 22 (2012) 16732–16737. doi:10.1039/C2JM32508J.

[54] H.M. Chen, R.-S. Liu, M.-Y. Lo, S.-C. Chang, L.-D. Tsai, Y.-M. Peng, J.-F. Lee, Hollow platinum spheres with nano-channels: Synthesis and enhanced catalysis for oxygen reduction, J. Phys. Chem. C. 112 (2008) 7522–7526. doi:10.1021/jp8017698.

[55] E. González, F. Merkoçi, R. Arenal, J. Arbiol, J. Esteve, N.G. Bastús, V. Puntes, Enhanced reactivity of high-index surface platinum hollow nanocrystals, J. Mater. Chem. A. 4 (2016) 200–208. doi:10.1039/C5TA07504A.

[56] F. Calle-Vallejo, J. Tymoczko, V. Colic, Q.H. Vu, M.D. Pohl, K. Morgenstern, D. Loffreda, P. Sautet, W. Schuhmann, A.S. Bandarenka, Finding optimal surface sites on heterogeneous catalysts by counting nearest neighbors, Science. 350 (2015) 185 LP-189. doi:10.1126/science.aab3501.

[57] J.R. Kitchin, J.K. Nørskov, M.A. Barteau, J.G. Chen, Role of strain and ligand effects in the modification of the electronic and chemical properties of bimetallic surfaces, Phys. Rev. Lett. 93 (2004) 156801. doi:10.1103/PhysRevLett.93.156801.

[58] V.R. Stamenkovic, B.S. Mun, M. Arenz, K.J.J. Mayrhofer, C.A. Lucas, G. Wang, P.N. Ross, N.M. Markovic, Trends in electrocatalysis on extended and nanoscale Pt-bimetallic alloy surfaces, Nat. Mater. 6 (2007) 241–247. doi:10.1038/nmat1840.

[59] J. Greeley, I.E.L. Stephens, A.S. Bondarenko, T.P. Johansson, H.A. Hansen, T.F. Jaramillo, J. Rossmeisl, I. Chorkendorff, J.K. Nørskov, Alloys of platinum and early transition metals as oxygen reduction electrocatalysts, Nat. Chem. 1 (2009) 552–556. doi:10.1038/nchem.367.

[60] M. Escudero-Escribano, P. Malacrida, M.H. Hansen, U.G. Vej-Hansen, A. Velázquez-Palenzuela, V. Tripkovic, J. Schiøtz, J. Rossmeisl, I.E.L. Stephens, I. Chorkendorff, Tuning the activity of Pt alloy electrocatalysts by means of the lanthanide contraction, Science. 352 (2016) 73–76. doi:10.1126/science.aad8892.

[61] N. Lindahl, E. Zamburlini, L. Feng, H. Grönbeck, M. Escudero-Escribano, I.E.L. Stephens, I. Chorkendorff, C. Langhammer, B. Wickman, High specific and mass activity for the oxygen reduction reaction for thin film catalysts of sputtered Pt_3Y, Adv. Mater. Interfaces. 4 (2017) 1700311. doi:10.1002/admi.201700311.

[62] V. Stamenkovic, B.S. Mun, K.J.J. Mayrhofer, P.N. Ross, N.M. Markovic, J. Rossmeisl, J. Greeley, J.K. Nørskov, Changing the activity of electrocatalysts for oxygen reduction by tuning the surface electronic structure, Angew. Chemie Int. Ed. 45 (2006) 2897–2901. doi:10.1002/anie.200504386.

[63] I.E.L. Stephens, A.S. Bondarenko, F.J. Perez-Alonso, F. Calle-Vallejo, L. Bech, T.P. Johansson, A.K. Jepsen, R. Frydendal, B.P. Knudsen, J. Rossmeisl, I. Chorkendorff, Tuning the activity of Pt(111) for oxygen electroreduction by subsurface alloying, J. Am. Chem. Soc. 133 (2011) 5485–5491. doi:10.1021/ja111690g.

[64] B. Hammer, K.W. Jacobsen, J.K. Nørskov, Role of nonlocal exchange correlation in activated adsorption, Phys. Rev. Lett. 70 (1993) 3971–3974. doi:10.1103/PhysRevLett.70.3971.

[65] Hammer B., Nørskov J.K. (1997) Theory of Adsorption and Surface Reactions. In: Lambert R.M., Pacchioni G. (eds) Chemisorption and reactivity on supported clusters and thin films. vol 331. Springer, Dordrecht.

[66] C. Wang, M. Chi, D. Li, D. van der Vliet, G. Wang, Q. Lin, J.F. Mitchell, K.L. More, N.M. Markovic, V.R. Stamenkovic, Synthesis of homogeneous Pt-bimetallic nanoparticles as highly efficient electrocatalysts, ACS Catal. 1 (2011) 1355–1359. doi:10.1021/cs200328z.

[67] C. Wang, M. Chi, G. Wang, D. Van Der Vliet, D. Li, K. More, H.H. Wang, J.A. Schlueter, N.M. Markovic, V.R. Stamenkovic, Correlation between surface chemistry and electrocatalytic properties of monodisperse Pt_xNi_{1-x} nanoparticles, Adv. Funct. Mater. 21 (2011) 147–152. doi:10.1002/adfm.201001138.

[68] J. Li, S. Sharma, J. Li, S. Sharma, X. Liu, Y. Pan, J.S. Spendelow, M. Chi, Y. Jia, P. Zhang, D.A. Cullen, Z. Xi, H. Lin, Z. Yin, B. Shen, M. Muzzio, C. Yu, Y.S. Kim, A.A. Peterson, K.L. More, H. Zhu, Advance fuel cell catalysis hard-magnet L10-CoPt nanoparticles advance fuel cell catalysis, Joule. 3 (2020) 124–135. doi:10.1016/j.joule.2018.09.016.

[69] P. Hernandez-Fernandez, F. Masini, D.N. McCarthy, C.E. Strebel, D. Friebel, D. Deiana, P. Malacrida, A. Nierhoff, A. Bodin, A.M. Wise, J.H. Nielsen, T.W. Hansen, A. Nilsson, I.E.L. Stephens, I. Chorkendorff, Mass-selected nanoparticles of Pt_xY as model catalysts for oxygen electroreduction, Nat. Chem. 6 (2014) 732–738. doi:10.1038/nchem.2001.

[70] A. Velázquez-Palenzuela, F. Masini, A.F. Pedersen, M. Escudero-Escribano, D. Deiana, P. Malacrida, T.W. Hansen, D. Friebel, A. Nilsson, I.E.L. Stephens, I. Chorkendorff, The enhanced activity of mass-selected Pt_xGd nanoparticles for oxygen electroreduction, J. Catal. 328 (2015) 297–307. doi:10.1016/j.jcat.2014.12.012.

[71] C. Cui, L. Gan, M. Heggen, S. Rudi, P. Strasser, Compositional segregation in shaped Pt alloy nanoparticles and their structural behaviour during electrocatalysis, Nat. Mater. 12 (2013) 765–771. doi:10.1038/nmat3668.

[72] S.-I. Choi, S. Xie, M. Shao, J.H. Odell, N. Lu, H.-C. Peng, L. Protsailo, S. Guerrero, J. Park, X. Xia, J. Wang, M.J. Kim, Y. Xia, Synthesis and characterization of 9 nm Pt-Ni octahedra with a record high activity of 3.3 A/mg_{Pt} for the oxygen reduction reaction, Nano Lett. 13 (2013) 3420–3425. doi:10.1021/nl401881z.

[73] X. Huang, L. Cao, Y. Chen, E. Zhu, Z. Lin, M. Li, A. Yan, A. Zettl, Y.M. Wang, X. Duan, T. Mueller, High-performance transition metal – doped Pt_3Ni octahedra for oxygen reduction reaction, Science. 348 (2015) 1230–1234. doi:10.1126/science.aaa8765

[74] C. Chen, Y. Kang, Z. Huo, Z. Zhu, W. Huang, H.L. Xin, J.D. Snyder, D. Li, J.A. Herron, M. Mavrikakis, M. Chi, K.L. More, Y. Li, N.M. Markovic, G.A. Somorjai, P. Yang, V.R. Stamenkovic, Highly crystalline multimetallic nanoframes with three-dimensional electrocatalytic surfaces, Science. 343 (2014) 1339 LP-1343. doi:10.1126/science.1249061.

[75] L. Bu, J. Ding, S. Guo, X. Zhang, D. Su, X. Zhu, J. Yao, J. Guo, G. Lu, X. Huang, A general method for multimetallic platinum alloy nanowires as highly active and stable oxygen reduction catalysts, Adv. Mater. 27 (2015) 7204–7212. doi:10.1002/adma.201502725.

[76] L. Bu, S. Guo, X. Zhang, X. Shen, D. Su, G. Lu, X. Zhu, J. Yao, J. Guo, X. Huang, Surface engineering of hierarchical platinum-cobalt nanowires for efficient electrocatalysis, Nat. Commun. 7 (2016) 11850. doi:10.1038/ncomms11850.

[77] S. Guo, D. Li, H. Zhu, S. Zhang, N.M. Markovic, V.R. Stamenkovic, S. Sun, FePt and CoPt nanowires as efficient catalysts for the oxygen reduction reaction, Angew. Chemie Int. Ed. 52 (2013) 3465–3468. doi:10.1002/anie.201209871.

[78] L. Bu, N. Zhang, S. Guo, X. Zhang, J. Li, J. Yao, T. Wu, G. Lu, J.-Y. Ma, D. Su, X. Huang, Biaxially strained PtPb/Pt core/shell nanoplate boosts oxygen reduction catalysis, Science. 354 (2016) 1410 LP-1414. doi:10.1126/science.aah6133.

[79] G.W. Sievers, A.W. Jensen, J. Quinson, A. Zana, F. Bizzotto, M. Oezaslan, A. Dworzak, J.J.K. Kirkensgaard, T.E.L. Smitshuysen, S. Kadkhodazadeh, M. Juelsholt, K.M.Ø. Jensen, K. Anklam, H. Wan, J. Schäfer, K. Čépe, M. Escudero-Escribano, J. Rossmeisl, A. Quade, V. Brüser, M. Arenz, Self-supported Pt–CoO networks combining high specific activity with high surface area for oxygen reduction, Nat. Mater. (2020). doi:10.1038/s41563-020-0775-8.

[80] L. Chong, J. Wen, J. Kubal, F.G. Sen, J. Zou, J. Greeley, M. Chan, H. Barkholtz, W. Ding, D.J. Liu, Ultralow-loading platinum-cobalt fuel cell catalysts derived from imidazolate frameworks, Science. 362 (2018) 1276–1281. doi:10.1126/science.aau0630.

[81] T. Yoshida, K. Kojima, Toyota MIRAI fuel cell vehicle and progress toward a future hydrogen society, Interface Mag. 24 (2015) 45–49. doi:10.1149/2.f03152if.

[82] F. Tao, S. Zhang, N. Luan, X. Zhang, Action of bimetallic nanocatalysts under reaction conditions and during catalysis: Evolution of chemistry from high vacuum conditions to reaction conditions, Chem. Soc. Rev. 41 (2012) 7980–7993. doi:10.1039/c2cs35185d.

[83] F. Tao, M.E. Grass, Y. Zhang, D.R. Butcher, J.R. Renzas, Z. Liu, J.Y. Chung, B.S. Mun, M. Salmeron, G.A. Somorjai, Reaction-driven restructuring of Rh-Pd and Pt-Pd core-shell nanoparticles, Science. 322 (2008) 932–934. doi:10.1126/science.1164170.

[84] M. Ahmadi, F. Behafarid, C. Cui, P. Strasser, B.R. Cuenya, Long-range segregation phenomena in shape-selected bimetallic nanoparticles: Chemical state effects, ACS Nano. 7 (2013) 9195–9204. doi:10.1021/nn403793a.

[85] L.-W. Wang, M. Salmeron, S. Alayoglu, H. Zheng, E.A. Stach, G.A. Somorjai, C.-M. Wang, L. Kovarik, H.L. Xin, A. Genc, R. Tao, Revealing the atomic restructuring of Pt–Co nanoparticles, Nano Lett. 14 (2014) 3203–3207. doi:10.1021/nl500553a.

[86] H. Topsøe, Developments in operando studies and in situ characterization of heterogeneous catalysts, J. Catal. 216 (2003) 155–164. doi:10.1016/S0021-9517(02)00133-1.

[87] X. Li, X. Yang, J. Zhang, Y. Huang, B. Liu, In situ/operando techniques for characterization of single-atom catalysts, ACS Catal. 9 (2019) 2521–2531. doi:10.1021/acscatal.8b04937.

[88] M. Tada, S. Murata, T. Asakoka, K. Hiroshima, K. Okumura, H. Tanida, T. Uruga, H. Nakanishi, S. Matsumoto, Y. Inada, M. Nomura, Y. Iwasawa, In situ time-resolved dynamic surface events on the Pt/C cathode in a fuel cell under operando conditions, Angew. Chemie Int. Ed. 46 (2007) 4310–4315. doi:10.1002/anie.200604732.

[89] M.A. Bañares, Operando methodology: combination of in situ spectroscopy and simultaneous activity measurements under catalytic reaction conditions, Catal. Today. 100 (2005) 71–77. doi:10.1016/j.cattod.2004.12.017.

[90] X. Deng, F. Galli, M.T.M. Koper, In situ electrochemical AFM imaging of a Pt electrode in sulfuric acid under potential cycling conditions, J. Am. Chem. Soc. 140 (2018) 13285–13291. doi:10.1021/jacs.8b07452.

[91] I. Khalakhan, A. Choukourov, M. Vorokhta, P. Kúš, I. Matolínová, V. Matolín, In situ electrochemical AFM monitoring of the potential-dependent deterioration of platinum catalyst during potentiodynamic cycling, Ultramicroscopy. 187 (2018) 64–70. doi:10.1016/j.ultramic.2018.01.015.

[92] L. Jacobse, Y.F. Huang, M.T.M. Koper, M.J. Rost, Correlation of surface site formation to nanoisland growth in the electrochemical roughening of Pt(111), Nat. Mater. 17 (2018) 277–282. doi:10.1038/s41563-017-0015-z.

[93] M. Ruge, J. Drnec, B. Rahn, F. Reikowski, D.A. Harrington, F. Carlà, R. Felici, J. Stettner, O.M. Magnussen, Structural reorganization of Pt(111) electrodes by electrochemical oxidation and reduction, J. Am. Chem. Soc. 139 (2017) 4532–4539. doi:10.1021/jacs.7b01039.

[94] Q. Xu, E. Kreidler, T. He, Performance and durability of PtCo alloy catalysts for oxygen electroreduction in acidic environments, Electrochim. Acta. 55 (2010) 7551–7557. doi:10.1016/j.electacta.2009.11.066.

[95] S. Nagashima, T. Ikai, Y. Sasaki, T. Kawasaki, T. Hatanaka, H. Kato, K. Kishita, Atomic-level observation of electrochemical platinum dissolution and redeposition, Nano Lett. 19 (2019) 7000–7005. doi:10.1021/acs.nanolett.9b02382.

[96] G.-Z. Zhu, S. Prabhudev, J. Yang, C.M. Gabardo, G.A. Botton, L. Soleymani, In situ liquid cell TEM study of morphological evolution and degradation of Pt–Fe nanocatalysts during potential cycling, J. Phys. Chem. C. 118 (2014) 22111–22119. doi:10.1021/jp506857b.

[97] J.A. Gilbert, N.N. Kariuki, R. Subbaraman, A.J. Kropf, M.C. Smith, E.F. Holby, D. Morgan, D.J. Myers, In situ anomalous small-angle x-ray scattering studies of platinum nanoparticle fuel cell electrocatalyst degradation, J. Am. Chem. Soc. 134 (2012) 14823–14833. doi:10.1021/ja3038257.

[98] M.C. Smith, J.A. Gilbert, J.R. Mawdsley, S. Seifert, D.J. Myers, In situ small-angle X-ray scattering observation of Pt catalyst particle growth during potential cycling, J. Am. Chem. Soc. 130 (2008) 8112–8113. doi:10.1021/ja801138t.

[99] J.A. Gilbert, N.N. Kariuki, X. Wang, A.J. Kropf, K. Yu, D.J. Groom, P.J. Ferreira, D. Morgan, D.J. Myers, Pt catalyst degradation in aqueous and fuel cell environments studied via in-operando anomalous small-angle X-ray acattering, Electrochim. Acta. 173 (2015) 223–234. doi:10.1016/j.electacta.2015.05.032.

[100] A. Witkowska, S. Dsoke, E. Principi, R. Marassi, A. Di Cicco, V. Rossi Albertini, Pt–Co cathode electrocatalyst behaviour viewed by in situ XAFS fuel cell measurements, J. Power Sources. 178 (2008) 603–609. doi:10.1016/j.jpowsour.2007.08.074.

[101] A.E. Russell, A. Rose, X-ray absorption spectroscopy of low temperature fuel cell catalysts, Chem. Rev. 104 (2004) 4613–4636. doi:10.1021/cr020708r.

[102] H. Imai, K. Izumi, M. Matsumoto, Y. Kubo, K. Kato, Y. Imai, In situ and real-time monitoring of oxide growth in a few monolayers at surfaces of platinum nanoparticles in aqueous media, J. Am. Chem. Soc. 131 (2009) 6293–6300. doi:10.1021/ja810036h.

[103] L. Nguyen, F.F. Tao, Y. Tang, J. Dou, X.-J. Bao, Understanding catalyst surfaces during catalysis through near ambient pressure X-ray photoelectron spectroscopy, Chem. Rev. 119 (2019) 6822–6905. doi:10.1021/acs.chemrev.8b00114.

[104] R. Mom, L. Frevel, J.-J. Velasco-Vélez, M. Plodinec, A. Knop-Gericke, R. Schlögl, The oxidation of platinum under wet conditions observed by electrochemical X-ray photoelectron spectroscopy, J. Am. Chem. Soc. 141 (2019) 6537–6544. doi:10.1021/jacs.8b12284.

[105] H.S. Casalongue, S. Kaya, V. Viswanathan, D.J. Miller, D. Friebel, H.A. Hansen, J.K. Nørskov, A. Nilsson, H. Ogasawara, Direct observation of the oxygenated species during oxygen reduction on a platinum fuel cell cathode, Nat. Commun. 4 (2013) 2817. doi:10.1038/ncomms3817.

[106] M. Favaro, C. Valero-Vidal, J. Eichhorn, F.M. Toma, P.N. Ross, J. Yano, Z. Liu, E.J. Crumlin, Elucidating the alkaline oxygen evolution reaction mechanism on platinum, J. Mater. Chem. A. 5 (2017) 11634–11643. doi:10.1039/C7TA00409E.

[107] I. Martens, R. Chattot, M. Rasola, M.V. Blanco, V. Honkimäki, D. Bizzotto, D.P. Wilkinson, J. Drnec, Probing the dynamics of platinum surface oxides in fuel cell catalyst layers using in situ X-ray diffraction, ACS Appl. Energy Mater. 2 (2019) 7772–7780. doi:10.1021/acsaem.9b00982.

[108] M. Nesselberger, M. Arenz, In situ FTIR spectroscopy: Probing the electrochemical interface during the oxygen reduction reaction on a commercial platinum high-surface-area catalyst, ChemCatChem. 8 (2016) 1125–1131. doi:10.1002/cctc.201501193.

[109] C. Lafforgue, F. Maillard, V. Martin, L. Dubau, M. Chatenet, Degradation of carbon-supported platinum-group-metal electrocatalysts in alkaline media studied by in situ fourier transform infrared spectroscopy and identical-location transmission electron microscopy, ACS Catal. 9 (2019) 5613–5622. doi:10.1021/acscatal.9b00439.

[110] A.K. Schuppert, A.A. Topalov, I. Katsounaros, S.O. Klemm, K.J.J. Mayrhofer, A scanning flow cell system for fully automated screening of electrocatalyst materials, J. Electrochem. Soc. 159 (2012) F670–F675. doi:10.1149/2.009211jes.

[111] O. Kasian, S. Geiger, K.J.J. Mayrhofer, S. Cherevko, Electrochemical on-line ICP-MS in electrocatalysis research, Chem. Rec. 19 (2019) 2130–2142. doi:10.1002/tcr.201800162.

[112] S. Cherevko, A.A. Topalov, A.R. Zeradjanin, G.P. Keeley, K.J.J. Mayrhofer, Temperature-dependent dissolution of polycrystalline platinum in sulfuric acid electrolyte, Electrocatalysis. 5 (2014) 235–240. doi:10.1007/s12678-014-0187-0.

[113] D.A. Cullen, M. Lopez-Haro, P. Bayle-Guillemaud, L. Guetaz, M.K. Debe, A.J. Steinbach, Linking morphology with activity through the lifetime of pretreated PtNi nanostructured thin film catalysts, J. Mater. Chem. A. 3 (2015) 11660–11667. doi:10.1039/c5ta01854d.

[114] N. Lindahl, B. Eriksson, H. Grönbeck, R.W. Lindström, G. Lindbergh, C. Lagergren, B. Wickman, Fuel cell measurements with cathode catalysts of sputtered Pt_3Y thin films, ChemSusChem. 11 (2018) 1438–1445. doi:10.1002/cssc.201800023.

[115] M. Cavarroc, A. Ennadjaoui, M. Mougenot, P. Brault, R. Escalier, Y. Tessier, J. Durand, S. Roualdès, T. Sauvage, C. Coutanceau, Performance of plasma sputtered fuel cell electrodes with ultra-low Pt loadings, Electrochem. Commun. 11 (2009) 859–861. doi:10.1016/j.elecom.2009.02.012.

[116] G. Sievers, S. Mueller, A. Quade, F. Steffen, S. Jakubith, A. Kruth, V. Brueser, Mesoporous Pt-Co oxygen reduction reaction (ORR) catalysts for low temperature proton exchange membrane fuel cell synthesized by alternating sputtering, J. Power Sources. 268 (2014) 255–260. doi:10.1016/j.jpowsour.2014.06.013.

[117] A.A. Fedotov, S.A. Grigoriev, E.K. Lyutikova, P. Millet, V.N. Fateev, Characterization of carbon-supported platinum nano-particles synthesized using magnetron sputtering for application in PEM electrochemical systems, Int. J. Hydrogen Energy. 38 (2013) 426–430. doi:10.1016/j.ijhydene.2012.09.121.

[118] R. Fiala, A. Figueroba, A. Bruix, M. Vaclavu, A. Rednyk, I. Khalakhan, M. Vorokhta, J. Lavkova, F. Illas, V. Potin, I. Matolinova, K.M. Neyman, V. Matolin, High efficiency of Pt^{2+}- CeO_2 novel thin film catalyst as anode for proton exchange membrane fuel cells, Appl. Catal. B Environ. 197 (2016) 262–270. doi:10.1016/j.apcatb.2016.02.036.

[119] A. Bruix, Y. Lykhach, I. Matolínová, A. Neitzel, T. Skála, N. Tsud, M. Vorokhta, V. Stetsovych, K. Ševčíková, J. Mysliveček, R. Fiala, M. Václavů, K.C. Prince, S. Bruyère, V. Potin, F. Illas, V. Matolín, J. Libuda, K.M. Neyman, Maximum noble-metal efficiency in catalytic materials: Atomically dispersed surface platinum, Angew. Chemie Int. Ed. 53 (2014) 10525–10530. doi:10.1002/anie.201402342.

[120] A. Ly, T. Asset, P. Atanassov, Integrating nanostructured Pt-based electrocatalysts in proton exchange membrane fuel cells, J. Power Sources. 478 (2020) 228516. doi:10.1016/j.jpowsour.2020.228516.

6. List of selected own publications

P-1. R. Fiala, M. Vaclavu, M. Vorokhta, I. Khalakhan, I. Matolinova, V. Matolin.
PEMFC made of magnetron sputtered Pt-CeO_x and Pt-Co thin film catalysts.
J. Power Sources, 2015, 273, 105-109
DOI: 10.1016/j.jpowsour.2014.08.093

P-2. M. Vorokhta, I. Khalakhan, M. Václavů, G. Kovács, S.M. Kozlov, P. Kúš, T. Skála, N. Tsud, J. Lavková, V. Potin, I. Matolínová, K.M. Neyman, V. Matolín.
Surface composition of magnetron sputtered Pt-Co thin film catalyst for proton exchange membrane fuel cells.
Appl. Surf. Sci., 2016, 365, 245–251
DOI: doi.org/10.1016/j.apsusc.2016.01.004

P-3. Khalakhan, L. Supik, M. Vorokhta, Y. Yakovlev, M. Dopita, D.J.S. Sandbeck, S. Cherevko, K. Veltruská, I. Matolínová.
Compositionally tuned magnetron co-sputtered Pt_xNi_{100-x} alloy as cathode catalyst for proton exchange membrane fuel cells.
Appl. Surf. Sci, 2020, 511, 145486
DOI: doi.org/10.1016/j.apsusc.2020.145486

P-4. R. Brown, M. Vorokhta, I. Khalakhan, M. Dopita, T. Vonderach, T. Skala, N. Lindahl, I. Matolinova, H. Grönbeck, K. Neyman, V. Matolin, B. Wickman.
Unravelling the surface chemistry and structure in highly active sputtered Pt_3Y catalyst films for the oxygen reduction reaction.
ACS Appl. Mater. Interfaces, 2020, 12(4), 4454-4462
DOI: doi.org/10.1021/acsami.9b17817

P-5. R. Brown, M. Vorokhta, T. Skála, I. Khalakhan, N. Lindahl, B. Eriksson, C. Lagergren, I. Matolínová, V. Matolín, B. Wickman.
Surface composition of a highly active Pt_3Y alloy catalyst for application in low temperature fuel cells.
Fuel cells, 2020, 20(4), 413-419
DOI: doi.org/10.1002/fuce.201900186

P-6. Khalakhan, M. Vorokhta, M. Václavů, B. Šmíd, J. Lavková, I. Matolínová, R. Fiala, N. Tsud, T. Skála, V. Matolín.
In-situ electrochemical atomic force microscopy study of aging of magnetron sputtered Pt-Co nanoalloy thin films during accelerated degradation test.
Electrochim. Acta, 2016, 211, 52-58
DOI: doi.org/10.1016/j.electacta.2016.06.035

P-7. Khalakhan, M. Vorokhta, P. Kúš, M. Dopita, M. Václavů, R. Fiala, N. Tsud, T. Skála, V. Matolín.
In situ probing of magnetron sputtered Pt-Ni alloy fuel cell catalysts during accelerated durability test using EC-AFM.
Electrochim. Acta, 2017, 245, 760–769
DOI: 10.1016/j.electacta.2017.05.202

P-8. Khalakhan, F. Waidhas, O. Brummel, M. Vorokhta, P. Kúš, Y.V. Yakovlev, M. Bertram, M. Dopita, I. Matolínová, J. Libuda, V. Matolín.
Nanoscale morphological and structural transformations of PtCu alloy electrocatalyst during potentiodynamic cycling.
J. Phys. Chem. C, 2018, 122 (38), 21974–21982
DOI: doi.org/10.1021/acs.jpcc.8b06840

P-9. O. Brummel, F. Waidhas, I. Khalakhan, M. Vorokhta, M. Dubau, G. Kovács, H.A. Aleksandrov, K.M. Neyman, V. Matolín, J. Libuda.
Structural transformations and adsorption properties of PtNi nanoalloy thin film electrocatalysts prepared by magnetron co-sputtering.
Electrochim. acta, 2017, 251, 427-441
DOI: doi.org/10.1016/j.electacta.2017.08.062

P-10. Khalakhan, A. Choukourov, M. Vorokhta, P. Kúš, I. Matolínová, V. Matolín.
In situ electrochemical AFM monitoring of the potential-dependent deterioration of platinum catalyst during potentiodynamic cycling.
Ultramicroscopy, 2018, 187, 64-70
DOI: doi.org/10.1016/j.ultramic.2018.01.015

P-11. M. Bogar, I. Khalakhan, A. Gambitta, Y. Yakovlev, H. Amenitsch.
In situ electrochemical grazing incidence small angle X-ray scattering: from the design of an electrochemical cell to an exemplary study of fuel cell catalyst degradation.
J. Power Sources, 2020, 477, 229030
DOI: doi.org/10.1016/j.jpowsour.2020.229030

P-12. Khalakhan, M. Bogar, M. Vorokhta, P. Kúš, Y. Yakovlev, M. Dopita, D. Sandbeck, S. Cherevko, I. Matolínová, H. Amenitsch.
Evolution of the PtNi bimetallic alloy fuel cell catalyst under simulated operational conditions.
ACS Appl. Mater. Interfaces, 2020, 12(15) 17602-17610
DOI: doi.org/10.1021/acsami.0c02083

P-13. Khalakhan, L. Vega, M. Vorokhta, T. Skála, F. Viñes, Y.V. Yakovlev, K.M. Neyman, I. Matolínová.
Irreversible structural dynamics on the surface of bimetallic PtNi alloy catalyst under alternating oxidizing and reducing environments.
Appl. Catal., B: Environmental, 2020, 264, 118476
DOI: doi.org/10.1016/j.apcatb.2019.118476